Tungsten–Carbon, Carbon–Hydrogen, and Carbon–Carbon Bond Activation in the Chemistry of 1,2-$W_2R_2(OR')_4$($W \equiv W$) Complexes. 1. Alkyne-Promoted Metal-to-Metal Alkyl Migrations, W≡W/C≡C Bond Metathesis, and Metallacyclopropene Formation

Malcolm H. Chisholm,* Bryan W. Eichhorn, Kirsten Folting, and John C. Huffman

Department of Chemistry and Molecular Structure Center, Indiana University, Bloomington, Indiana 47405

Received February 1, 1988

Compounds of formula 1,2-W_2R_2(O-*i*-Pr)$_4$($W \equiv W$) (1) (where R = Me, Et, CH_2Ph, CH_2SiMe_3, *n*-Pr, *i*-Bu, C_6H_5, and C_6H_4-*p*-Me) react with internal acetylenes (MeC≡CMe, MeC≡CEt, and EtC≡CEt) in hydrocarbon solvents to form bis(alkyne) adducts of formula $W_2R_2(R'CCR'')_2$(O-*i*-Pr)$_4$ (**2**) in good yields. Similarly 1,2-$W_2(C_6H_4$-*p*-Me$)_2$(O-*t*-Bu)$_4$ reacts with MeC≡CMe (2 equiv) to form $W_2(C_6H_4$-*p*-Me$)_2$-(MeCCMe)$_2$(O-*t*-Bu)$_4$ (**2'**). Compounds **2** and **2'** were characterized by ^{1}H NMR, ^{13}C NMR, IR, and electronic absorption spectroscopy and elemental analysis. Single-crystal X-ray diffraction studies of $W_2(C_6H_5)_2$-(MeCCMe)$_2$(O-*i*-Pr)$_4$ and $W_2(CH_2Ph)_2$(MeCCMe)$_2$(O-*i*-Pr)$_4$ revealed puckered $W_2(\mu$-O-*i*-Pr$)_2$ cores with M–M distances of 2.66 (1) and 2.67 (1) Å, respectively. The coordinated alkyne ligands display short W–C distances (2.05 (2) Å) and long C–C distances (1.31 (2) Å) and are best viewed as metallacyclopropene units. The unusual molecular geometries of compounds **2** and **2'** are attributed to optimization of M–L π bonding at the expense of M–M bonding based on the findings of a qualitative molecular orbital analysis. The barriers to alkyne rotation about the metal–alkyne vectors ($\Delta G^{\ddagger}$) were calculated to be ca. 9.6 kcal mol^{-1} for compound **2** and 14.4 kcal mol^{-1} for compound **2'**. The barrier to rotation about the W–C(Ar) bond ($\Delta G^{\ddagger}$) in **2** (R = C_6H_4-*p*-Me, R' = R'' = Me) was calculated to be 7.5 (3) kcal mol^{-1} at −130 °C indicative of no significant metal-to-arene π* back-bonding. Ethyne, terminal and diphenylacetylenes do not react with compounds **1** apparently due to the poorer basicity of these alkynes relative to MeC≡CMe, MeC≡CEt, and EtC≡CEt. The Mo analogues of **1** do not form analogous bis(alkyne) compounds **2** but act as alkyne polymerization catalysts. The lack of reactivity in the Mo system is attributed to a mismatch of orbital energies between the acetylene π* orbitals and the filled Mo d orbitals. 1,2-$W_2(CH_2$-*t*-Bu$)_2$(O-*i*-Pr)$_4$ reacts with EtC≡CEt to form [W(≡CEt)(CH_2-*t*-Bu)(O-*i*-Pr$)_2]_2$ (**4**) in a 64% isolated yield. This reaction represents a W≡W/C≡C bond metathesis that overrides the formation of compounds **2** when the steric demands of the system become sufficiently large. An X-ray diffraction study of **4** revealed a dimeric molecular structure in which the two TBP metal atoms are fused along a common axial–equatorial edge by virtue μ-O-*i*-Pr bridges with a W≡C distance of 1.76 (2) Å and a W–W separation of 3.514 (1) Å. In solution, **4** was shown to be in equilibrium with the monomeric compound W(≡CEt)(CH_2-*t*-Bu)(O-*i*-Pr$)_2$ (**4'**). Compound **4** reacts with pyridine (py) to form a py adduct of formula [W(≡CEt)(CH_2-*t*-Bu)(O-*i*-Pr$)_2$(py)$]_2$ (**5**). The proposed structure of **5** consists of an edge-shared bioctahedral geometry in which the py ligands are trans to the CH_2-*t*-Bu groups. 1,2-W_2Me_2(O-*t*-Bu)$_4$(py)$_2$ reacts with MeC≡CMe to form 1,1-$W_2Me_2(\mu$-$C_2Me_2)$(O-*t*-Bu)$_4$(py) (**6**) representing the first fully characterized example of a metal-to-metal alkyl migration on a W_2 center. In the solid state, **6** contains a slightly skewed alkyne bridge and no molecular symmetry. In solution, a turnstile rotation presumably occurs about one end of the molecule generating an apparent plane of symmetry. 1,2-W_2Me_2(O-*t*-Bu)$_4$(py)$_2$ reacts with ethyne to form $W_2Me(\mu$-HCCH)(O-*t*-Bu)$_5$(py) in low yield presumably by intermolecular ligand group scrambling. Crystal data for $W_2(CH_2Ph)_2$(O-*i*-Pr)$_4$(MeCCMe)$_2$ at −159 °C: a = 11.999 (2) Å, b = 18.650 (4) Å, c = 15.522 (3) Å, β = 97.84 (1)°, Z = 4, d_{calcd} = 1.727 g cm^{-3}, and space group $P2_1/n$. For $W_2(Ph)_2$(O-*i*-Pr)$_4$(MeCCMe)$_2$ at −159 °C: a = 11.854 (2) Å, b = 19.543 (4) Å, c = 14.699 (2) Å, β = 105.70 (1)°, Z = 4, d_{calcd} = 1.756 g cm^{-3}, and space group $P2_1/n$. For W_2Me_2(O-*t*-Bu)$_4$(py)(MeCCMe) at −162 °C: a = 9.468 (3) Å, b = 35.968 (16) Å, c = 10.176 (3) Å, β = 113.68 (2)°, Z = 4, d_{calcd} = 1.724 g cm^{-3}, and space group $P2_1/c$. For [W(≡CEt)(O-*i*-Pr$)_2$(CH_2-*t*-Bu)$]_2$ at −155 °C: a = 9.947 (2) Å, b = 10.481 (2) Å, c = 9.457 (2) Å, α = 93.40 (1)°, β = 108.07 (1)°, γ = 107.66 (1)°, Z = 1, d_{calcd} = 1.563 g cm^{-3}, and space group $P\bar{1}$.

Introduction

Much of organometallic chemistry can be categorized according to the inorganic template. For example, square-planar d^8 metal complexes such as Wilkinson's compound, Vaska's compound, and organoplatinum(II) and palladium(II) complexes share common modes of reactivity that are merely modified by the metal, its oxidation state, and supporting ligands.[1] An alternate classification of reaction chemistry can be developed from a fragment molecular orbital approach.[2] For example, the chemistry of the bent Cp_2M or Cp^*_2M fragment (Cp = η^5-C_5H_5 and Cp* = η^5-C_5Me_5) has dominated the development of the organometallic chemistry of the early transition elements,[3] the early actinides[4] and lanthanides.[5] Within this framework we are trying to develop the chemistry associated with compounds containing a central $(M \equiv M)^{6+}$ unit where M = Mo and W.[6] These d^3–d^3 dinuclear compounds provide an active center for reductive-elimination and oxidative-addition reactions.[6,7] The

(1) This represents a ligand field approach and is exemplified by the 16–18 electron rule: Tolman, C. A. *Chem. Soc. Rev.* **1972**, *1*, 337.
(2) (a) Hoffmann, R. *Angew. Chem.* **1982**, *94*, 725; *Angew. Chem. Int. Ed. Engl.* **1982**, *21*, 711. (b) Albright, T. A.; Burdett, J. K.; Whangbo, M.-H. In *Orbital Interactions in Chemistry*; Wiley: New York, 1985.
(3) Wolczanski, P. T.; Bercaw, J. E. *Acc. Chem. Res.* **1980**, *13*, 121.
(4) Marks, T. J. *Science (Washington, D.C.)* **1982**, *217*, 989.
(5) (a) Evans, W. J. *Polyhedron* **1987**, *6*, 803. (b) Bercaw, J. E.; Thompson, M. E. *Pure Appl. Chem.* **1984**, *56*, 1. (c) Andersen, R. A.; Tilley, T. D. *Inorg. Chem.* **1981**, *20*, 3627.
(6) Chisholm, M. H. *Angew. Chem.* **1986**, *98*, 21; *Angew. Chem., Int. Ed. Engl.* **1986**, *25*, 21.

0276-7333/89/2308-0049$01.50/0

M–M triple bond of configuration $\sigma^2\pi^4$ is tunable by the attendant ligands[8] and may be interconverted with different M–M MO valence configurations, e.g. $\pi^4\delta^2$ and $\sigma^2\pi^2\delta^2$ or $\sigma^2\pi^2\delta^{*2}$.[9-11]

A particularly attractive group of d^3–d^3 dinuclear compounds are the alkoxides of formula $(RO)_3M{\equiv}M(OR)_3$.[12-14] Here the M–M π and σ orbitals lie roughly 2 eV higher in energy than the oxygen lone pairs (M–OR π bonds), and the vacant frontier MOs are metal-centered δ/δ^*-type orbitals, the M–OR π^* orbitals.[8,15,16] The metal atoms may be viewed as electronically π-buffered and attain a share of 18 valence electrons by virtue of oxygen-to-metal π bonding although the M–OR π electrons are mainly ligand centered. Consequently the $M_2(OR)_6$ compounds are capable of undergoing Lewis base association reactions of the type shown in eq 1.[14]

$$M_2(OR)_6 + 2L \rightleftharpoons M_2(OR)_6L_2 \quad (1)$$

The position of equilibrium in eq 1 is dependent upon the metal, Mo vs W, the nature of the ligand L, and the alkoxide OR. Since the M≡M bond in $M_2(OR)_6$ compounds serves as a reservoir of electrons, the addition of unsaturated organic molecules to $M_2(OR)_6$ compounds provides an entry into an organometallic chemistry supported by the $M_2(OR)_6$ fragment in a manner not unlike that of Cp_2Ti or Cp^*_2Zr. The addition of alkynes or ethylene has been noted to lead to C–C coupling reactions, e.g., as in the formation of $W_2(OR)_6(\mu\text{-}C_4R_4')(C_2R_2')$, where R = *i*-Pr or CH_2-*t*-Bu and R′ = H or Me,[17] and $W_2(O\text{-}i\text{-}Pr)_6(CH_2)_4(C_2H_4)$[18] and $W_2(O\text{-}i\text{-}Pr)_6(\mu\text{-}CCH_2CH_2CH_2)$ compounds.[19] In general there is a tendency for the $(M{\equiv}M)^{6+}$ unit to be oxidized by π-acidic ligands to $(M{=}M)^{8+}$ and $(M{-}M)^{10+}$ with the formation of new metal–ligand bonds. In certain cases the $(M{\equiv}M)^{6+}$ unit can be cleaved in a formal six-electron oxidation. This was first noted by Schrock and co-workers[20] in the reactions involving $W_2(O\text{-}t\text{-}Bu)_6$ with certain alkynes and nitriles (eq 2 and 3).

$$W_2(O\text{-}t\text{-}Bu)_6 + RC{\equiv}CR \rightarrow 2(t\text{-}BuO)_3W{\equiv}CR \quad (2)$$

R = Me, Et, Pr

$$W_2(O\text{-}t\text{-}Bu)_6 + RC{\equiv}N \rightarrow (t\text{-}BuO)_3W{\equiv}N + (t\text{-}BuO)_3W{\equiv}CR \quad (3)$$

R = Me, Ph

Subsequent work showed that reactions of type 2 and 3 were not limited to $W_2(O\text{-}t\text{-}Bu)_6$[21,22] and that reactions involving alkynes and $W_2(OR)_6$ compounds were sensitive to a variety of steric and electronic factors.[23]

We recently reported the preparation and characterization of complexes of formula $R'(RO)_2M{\equiv}M(OR)_2R'$ (hereafter referred to as 1,2-$M_2R_2'(OR)_4$) and $R'(RO)_2M{\equiv}M(OR)_3$ where M = Mo[24] and W[25] and R′ = an alkyl or aryl ligand. These compounds contain M–C σ bonds in addition to the previously noted desirable features associated with $(RO)_3M{\equiv}M(OR)_3$ compounds. They therefore pose as fascinating starting materials for the study of organometallic chemistry supported by the $(M{\equiv}M)^{6+}$ unit. The hydrocarbyl ligand R′ affects the organometallic chemistry of the $(M{\equiv}M)^{6+}$ unit as both a spectator and an active participant, thereby illiciting reactivity inaccessible to the $M_2(OR)_6$ compounds.

In this paper we describe the synthesis and characterization of certain compounds formed from the reactions between 1,2-$M_2R_2'(OR)_4(M{\equiv}M)$ compounds and alkynes. These are derived from metal-to-metal alkyl migrations, W≡W and C≡C bond metathesis, and metallacyclopropene formation. In the following paper,[26a] we describe the synthesis and characterization of dinuclear alkylidyne hydride and alkylidyne alkyl complexes formed by competitive alkane and dihydrogen elimination processes involving the metallacyclopropene complexes reported here. In the third paper,[26b] we describe competitive α- and β-hydrogen activation processes involving 1,2-$W_2R_2'(OR)_4$ compounds in their reactions with alkynes. A preliminary report of some of this work has appeared.[27]

Syntheses

General Considerations. Alkynes and 1,2-$W_2R_2(OR')_4(W{\equiv}W)$ compounds react in a variety of ways to form numerous different products. The modes of reaction are dependent upon the steric constraints of the alkyne and alkoxide ligands and the nature of the alkyl ligand R (i.e. β- or non-β-hydrogen-containing alkyls). In addition, the relative orbital energies of the alkyne π orbitals also affect the course of reaction. Scheme I summarizes some of the chemistry supported by these systems. In this and the following two papers, these reactions will be described individually and the factors influencing the various modes of reaction will be discussed.

1,2-$W_2R_2(R'CCR'')_2(O\text{-}i\text{-}Pr)_4$ and 1,2-$W_2(C_6H_4\text{-}p\text{-}Me)_2(MeCCMe)_2(O\text{-}t\text{-}Bu)_4$. Compounds of formula 1,2-$W_2R_2(O\text{-}i\text{-}Pr)_4(W{\equiv}W)$ (1), where R = Me, Et, CH_2Ph, CH_2SiMe_3, *n*-Pr, *i*-Bu, C_6H_5, and C_6H_4-*p*-Me, react with internal acetylenes (MeC≡CMe, MeC≡CEt, or EtC≡CEt) in alkane or ethereal solvents to form bis(alkyne) adducts of formula 1,2-$W_2R_2(R'CCR'')_2(O\text{-}i\text{-}Pr)_4$ (2) according to eq 4. These reactions are rapid at 0 °C ($t_{1/2}$

(7) Chisholm, M. H. *Polyhedron* **1986**, *5*, 25.
(8) This is well evident from He I and He II photoelectron spectra of $M_2(OR)_6$ compounds: Kober, E. M.; Lichtenberger, D. L. *J. Am. Chem. Soc.* **1985**, *107*, 7199.
(9) Chisholm, M. H.; Clark, D. L.; Huffman, J. C.; Van Der Sluys, W. G.; Kober, E. M.; Lichtenberger, D. L.; Bursten, B. E. *J. Am. Chem. Soc.* **1987**, *109*, 6796.
(10) Chisholm, M. H.; Clark, D. L.; Huffman, J. C.; Van Der Sluys, W. G. *J. Am. Chem. Soc.* **1987**, *109*, 6817.
(11) Cotton, F. A. *Polyhedron* **1987**, *6*, 667.
(12) Chisholm, M. H.; Cotton, F. A.; Murillo, C. A.; Reichert, W. W. *Inorg. Chem.* **1977**, *16*, 1801.
(13) Akiyama, M.; Chisholm, M. H.; Cotton, F. A.; Haitko, D. A.; Extine, M. W.; Little, D.; Fanwick, P. E. *Inorg. Chem.* **1979**, *18*, 2266.
(14) Chisholm, M. H. *Polyhedron* **1983**, *2*, 681.
(15) Cotton, F. A.; Stanley, G. G.; Kalbacher, B.; Green, J. C.; Seddon, E.; Chisholm, M. H. *Proc. Natl. Acad. Sci. U.S.A.* **1977**, 3109.
(16) Chisholm, M. H.; Clark, D. L.; Kober, E. M.; Van Der Sluys, W. G. *Polyhedron* **1987**, *6*, 723.
(17) Chisholm, M. H.; Hoffman, D. M.; Huffman, J. C. *J. Am. Chem. Soc.* **1984**, *106*, 6806.
(18) Chisholm, M. H.; Hampden-Smith, M.; Huffman, J. C., submitted for publication in *J. Am. Chem. Soc.*
(19) Chisholm, M. H.; Hampden-Smith, M. *J. Am. Chem. Soc.* **1987**, *109*, 5871.
(20) Schrock, R. R.; Listemann, M. L.; Sturgeoff, L. G. *J. Am. Chem. Soc.* **1982**, *104*, 4291.
(21) Schrock, R. R.; Listemann, M. L. *Organometallics* **1985**, *4*, 74.
(22) Schrock, R. R.; Strutz, H. *Organometallics* **1984**, *3*, 1600.
(23) Chisholm, M. H.; Conroy, B. K.; Eichhorn, B. W.; Folting, K.; Hoffman, D. M; Huffman, J. C.; Marchant, N. S. *Polyhedron* **1987**, *6*, 783 and references therein.
(24) Chisholm, M. H.; Tatz, R. J. *Organometallics* **1986**, *5*, 1590.
(25) Chisholm, M. H.; Eichhorn, B. W.; Folting, K.; Huffman, J. C.; Tatz, R. J. *Organometallics* **1986**, *5*, 1599.
(26) (a) Chisholm, M. H.; Eichhorn, B. W.; Huffman, J. C. *Organometallics*, second of three papers in this issue. (b) Chisholm, M. H.; Eichhorn, B. W.; Huffman, J. C. *Organometallics*, third of three papers in this issue.
(27) Chisholm, M. H.; Eichhorn, B. W.; Huffman, J. C. *J. Chem. Soc., Chem. Commun.* **1985**, 861.

$$\underset{\mathbf{1}}{1,2\text{-}W_2R_2(O\text{-}i\text{-}Pr)_4} + 2R'C{\equiv}CR'' \rightarrow \underset{\mathbf{2}}{W_2R_2(R'CCR'')_2(O\text{-}i\text{-}Pr)_4} \quad (4)$$

R = CH_2Ph, *i*-Bu, *n*-Pr; R′ or R″ = Me or Et

R = Me, CH_2SiMe_3; R′ = R″ = Me or Et

R = Et, C_6H_5, C_6H_4-*p*-Me; R′ = R″ = Me

< 5 s), but in certain cases (R = C_6H_5, CH_2Ph, C_6H_4-*p*-Me, *n*-Pr) transient green colors are observed in the conversion of brownish orange (1) to orange (2). The green intermediates may be monoalkyne adducts (cf. green $W_2(\mu\text{-}C_2H_2)(O\text{-}t\text{-}Bu)_6(py)$),[28] but attempts to trap or isolate these compounds or detect them spectroscopically have been unsuccessful thus far. When reaction 4 is carried out with less than 2 equiv of acetylene, only mixtures of unreacted $W_2R_2(O\text{-}i\text{-}Pr)_4$ and 2 are observed. The bis(alkyne) adducts 2 adopt a common structure, depicted by I, which

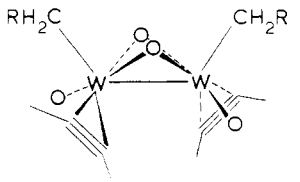

I, O = alkoxide

will be discussed in detail later. Compounds 2 have been characterized by elemental analysis (when possible), variable-temperature ^1H and ^{13}C NMR, IR, and electronic absorption spectroscopy, and two examples have been characterized by X-ray crystallography. The source of the $1,2\text{-}W_2R_2(O\text{-}i\text{-}Pr)_4$ substrate (1) in eq 4 is dependent upon the steric properties of the R group. The aryl isopropoxide complexes of 1 (R = C_6H_5, C_6H_4-*p*-Me) exist as mono-$HNMe_2$ adducts in the solid state and as stable, base-free $1,2\text{-}W_2R_2(O\text{-}i\text{-}Pr)_4$ species in hydrocarbon solutions.[25] For R = CH_2Ph, *i*-Bu, and CH_2SiMe_3, the base-free $W_2R_2(O\text{-}i\text{-}Pr)_4$ complexes are isolable and relatively thermally stable[25] in solution whereas for R = *n*-Pr, Et, and Me, the compounds 1 are thermally unstable and must be generated in situ from the corresponding $W_2R_2(NMe_2)_4$ precursors immediately prior to use. Because of the high reactivity of "$W_2Me_2(O\text{-}i\text{-}Pr)_4$", protolysis of the W–Me bond by *i*-PrOH is facile and small quantities of $W_2(O\text{-}i\text{-}Pr)_6(HNMe_2)_2$ are always generated in solution during isopropyl alcoholysis. This hexaalkoxide contaminate reacts to form alkylidyne impurities $[W(\equiv CR')(O\text{-}i\text{-}Pr)_3(HNMe_2)]_2$ (where R′ = Me or Et)[29] that are difficult to separate from the desired product 2.

The bis(alkyne) adducts 2 can be isolated from hydrocarbon solutions as brown-orange crystalline compounds that are stable under N_2 atmospheres and moderately stable in air for short periods of time. All are very soluble in hydrocarbon and ethereal solvents, and the benzyl derivatives (R = CH_2Ph) are thermochromic in frozen toluene solutions turning from orange to forest green below ca. −140 °C. All compounds 2 are unreactive toward Lewis bases such as PMe_3, py, or additional equivalents of alkyne. In solution, the alkyl derivatives of 2 are thermally and photochemically susceptible to C–H bond activation of the hydrocarbyl ligands. The decomposition products and mechanisms of decomposition are dramatically dependent upon the nature of R, and a detailed description of these hydrocarbyl degradation pathways is presented in the following two papers of this issue.

$W_2(C_6H_4\text{-}p\text{-}Me)_2(O\text{-}t\text{-}Bu)_4$ reacts with 2-butyne (2 equiv) in hexane solutions to form the bis(alkyne) adduct $W_2(C_6H_4\text{-}p\text{-}Me)_2(MeCCMe)_2(O\text{-}t\text{-}Bu)_4$ (2′) in high yield. Compound 2′ also adopts a structure depicted by I, like compounds 2, and is the only O-*t*-Bu substituted member in the series of bis(alkyne) complexes. The physical properties of 2′ are quite similar to those of 2 just described.

The reactions involving alkynes and $1,2\text{-}W_2(CH_2\text{-}t\text{-}Bu)_2(O\text{-}i\text{-}Pr)_4$ are surprisingly different from those observed for the other hydrocarbyl alkoxide complexes 1 just described. The anomalous reactivity of this compound is apparently due to the excessive steric demands of the bulky neopentyl ligand. The reaction between $1,2\text{-}W_2(CH_2\text{-}t\text{-}Bu)_2(O\text{-}i\text{-}Pr)_4$ and 2-butyne (eq 4, R′ = R″ = Me) does *not* yield the analogous bis(alkyne) adduct 2 but instead produces an alkyne-coupled, alkylidyne hydride complex of formula $HW_2(\mu\text{-}C\text{-}t\text{-}Bu)(\mu\text{-}C_4Me_4)(O\text{-}i\text{-}Pr)_4$ (3) and 1 equiv of neopentane according to eq 5. Although

$$\underset{\mathbf{1}}{W_2(CH_2\text{-}t\text{-}Bu)_2(O\text{-}i\text{-}Pr)_4} + 2MeC{\equiv}CMe \rightarrow \underset{\mathbf{3}}{HW_2(\mu\text{-}C\text{-}t\text{-}Bu)(\mu\text{-}C_4Me_4)(O\text{-}i\text{-}Pr)_4} + CMe_4 \quad (5)$$

compound 2 cannot be isolated or detected spectroscopically when R = CH_2-*t*-Bu, it is most likely an intermediate in the formation of 3. The synthesis and characterization of 3 and mechanistic details of the thermal and photochemical conversion of 2 to related μ-alkylidyne hydrido complexes are presented in the following paper.

The $1,2\text{-}W_2R_2(O\text{-}i\text{-}Pr)_4$ compounds (1) are surprisingly *unreactive* toward HC≡CH, HC≡CPh, PhC≡CPh, and $Me_3SiC{\equiv}CSiMe_3$ and no analogues of 2 with R′ or R″ = H, Ph, or $SiMe_3$ have been detected. The lack of reactivity of $Me_3SiC{\equiv}CSiMe_3$ presumably originates from steric factors whereas ethyne and the phenylacetylenes do not react for electronic reasons. PES data[30] for HCCH and PhCCPh reveal a ca. 2 eV stabilization of the acetylenic π electrons, relative to MeCCMe, rendering them less basic and therefore less reactive. However, the terminal acetylenes HCCH and HCCPh undergo slow proton-transfer reactions with $W_2(CH_2Ph)_2(O\text{-}i\text{-}Pr)_4$ producing toluene and as yet unidentified mixtures of organometallic products. The proton source in these reactions is the "acidic" C≡C—*H* hydrogen as determined by deuterium-labeling studies.

The molybdenum analogues of 1, $1,2\text{-}Mo_2R_2(O\text{-}i\text{-}Pr)_4$, do *not* form analogous alkyne adducts 2 but instead act as alkyne polymerization catalysts to form polyacetylenes. The difference in reactivities between corresponding Mo and W complexes is most likely due to unfavorable orbital energetics between the acetylene π^* and filled Mo d orbitals. These interactions will be discussed in detail later.

$[W(\equiv CEt)(CH_2\text{-}t\text{-}Bu)(O\text{-}i\text{-}Pr)_2]_2$ and py Adducts. The reaction between $1,2\text{-}W_2(CH_2\text{-}t\text{-}Bu)_2(O\text{-}i\text{-}Pr)_4$ and 3-hexyne follows yet another reaction pathway (eq 6) involving W≡W and C≡C bond metathesis to form $[W(\equiv CEt)(CH_2\text{-}t\text{-}Bu)(O\text{-}i\text{-}Pr)_2]_2$ (4) as the only observable organometallic product. The formation of 4 in preference to the bis(alkyne) adduct 2 appears to result from steric

$$\underset{\mathbf{1}}{W_2(CH_2\text{-}t\text{-}Bu)_2(O\text{-}i\text{-}Pr)_4} + EtC{\equiv}CEt \rightarrow \underset{\mathbf{4}}{[W(\equiv CEt)(CH_2\text{-}t\text{-}Bu)(O\text{-}i\text{-}Pr)_2]_2} \quad (6)$$

(28) Chisholm, M. H.; Folting, K.; Hoffman, D. M.; Huffman, J. C. *J. Am. Chem. Soc.* **1984**, *106*, 6794.

(29) Chisholm, M. H.; Conroy, B. K.; Huffman, J. C. *Organometallics* **1986**, *5*, 2384.

(30) Turner, D. W.; Baker, C.; Baker, A. D.; Brundle, C. R. *Molecular Photoelectron Spectroscopy*; Wiley-Interscience: London, 1970.

Scheme I

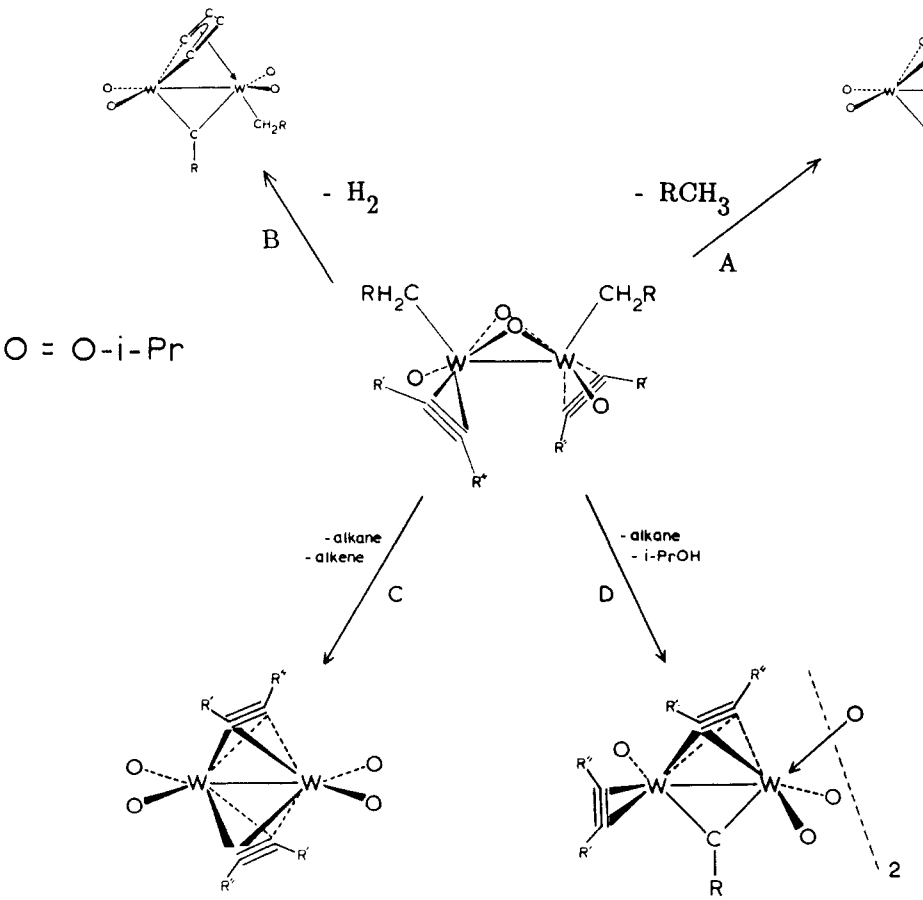

Table I. Selected Bond Distances (Å) and Angles (deg) for $W_2(CH_2Ph)_2(MeCCMe)_2(O\text{-}i\text{-}Pr)_4$

Bond Distances			
W(1)–W(2)	2.6684 (6)	W(2)–O(11)	2.140 (4)
W(1)–O(3)	1.856 (4)	W(2)–O(15)	2.070 (4)
W(1)–O(11)	2.074 (4)	W(2)–O(33)	1.857 (4)
W(1)–O(15)	2.167 (4)	W(2)–C(26)	2.208 (7)
W(1)–C(8)	2.061 (7)	W(2)–C(38)	2.051 (6)
W(1)–C(9)	2.043 (6)	W(2)–C(39)	2.048 (8)
W(1)–C(19)	2.213 (7)	C(8)–C(9)	1.296 (9)
		C(38)–C(39)	1.323 (10)

Bond Angles			
W(2)–C(1)–O(3)	115.89 (13)	O(15)–W(2)–C(26)	89.90 (22)
W(2)–W(1)–C(19)	123.54 (18)	O(33)–W(2)–C(26)	102.65 (23)
O(3)–W(1)–O(11)	91.01 (18)	W(1)–O(3)–C(4)	137.8 (4)
O(3)–W(1)–C(19)	106.25 (21)	W(1)–O(11)–W(2)	78.55 (14)
O(11)–W(1)–C(19)	93.67 (22)	W(1)–O(15)–W(2)	78.02 (14)
O(15)–W(1)–C(19)	80.61 (20)	W(2)–O(33)–C(34)	145.3 (4)
W(1)–W(2)–O(33)	115.51 (14)	C(7)–C(8)–C(9)	135.8 (7)
W(1)–W(2)–C(26)	123.15 (18)	C(8)–C(9)–C(10)	139.6 (7)
O(11)–W(2)–C(26)	81.99 (21)	C(37)–C(38)–C(39)	140.1 (7)
O(15)–W(2)–O(33)	89.01 (18)	C(38)–C(39)–C(40)	136.9 (7)

constraints at the metal center and not electronic properties of the alkyl ligands. Reaction 6 represents a net six-electron reduction of EtC≡CEt, and it can therefore be assumed that better electron-donor substituents on the W_2 center would favor this reaction over alkyne adduct formation of eq 4. However, a comparison of the inductive or polar parameters (Taft's constants)[31] of CH_2SiMe_3 versus CH_2-*t*-Bu reveals that CH_2SiMe_3 is a significantly better electron-releasing group. As previously mentioned, 1,2-$W_2(CH_2SiMe_3)_2(O\text{-}i\text{-}Pr)_4$ reacts with EtC≡CEt to form **2** (R = CH_2SiMe_3, R′ = R″ = Et) and no analogue of **4** with R = CH_2SiMe_3 has been detected. Thus, it appears that the preference for reaction 6 over reaction 4 using EtC≡CEt results from the steric demands of the alkyl ligands (CH_2-*t*-Bu > CH_2SiMe_3) and not their electronic (inductive) properties.

Compound **4** can be isolated in good yield as pale yellow crystals from pentane and is very air-sensitive and somewhat thermally unstable in solution and in the crystalline state. In the solid state, **4** exists as a weakly associated dimer, depicted by II, and in toluene, a monomer–dimer

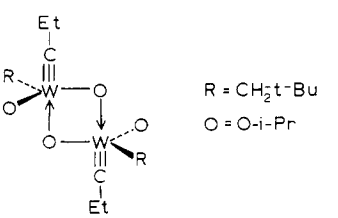

II

equilibrium is established (eq 7). This has been monitored

$$[W(\equiv CEt)(CH_2\text{-}t\text{-}Bu)(O\text{-}i\text{-}Pr)_2]_2 \rightleftharpoons \underset{4}{} \quad 2W(\equiv CEt)(CH_2\text{-}t\text{-}Bu)(O\text{-}i\text{-}Pr)_2 \quad (7)$$
$$\underset{4'}{}$$

by ^1H NMR as a function of temperature. Compound **4** reacts with pyridine (py) in hexane solutions to form the pyridine adduct $[W(\equiv CEt)(CH_2\text{-}t\text{-}Bu)(O\text{-}i\text{-}Pr)_2(py)]_2$ (**5**) according to eq 8. This compound can be isolated from

$$W(\equiv CEt)(CH_2\text{-}t\text{-}Bu)(O\text{-}i\text{-}Pr)_2 + py \rightarrow \underset{4}{} \quad \tfrac{1}{2}[W(\equiv CEt)(CH_2\text{-}t\text{-}Bu)(O\text{-}i\text{-}Pr)_2(py)]_2 \quad (8)$$
$$\underset{5}{}$$

hexane as thermally sensitive, pale-brown crystals and is

(31) Lowry, J. H.; Richardson, K. S. *Mechanisms and Theory in Organic Chemistry*; Harper and Row: New York, 1981; p 138.

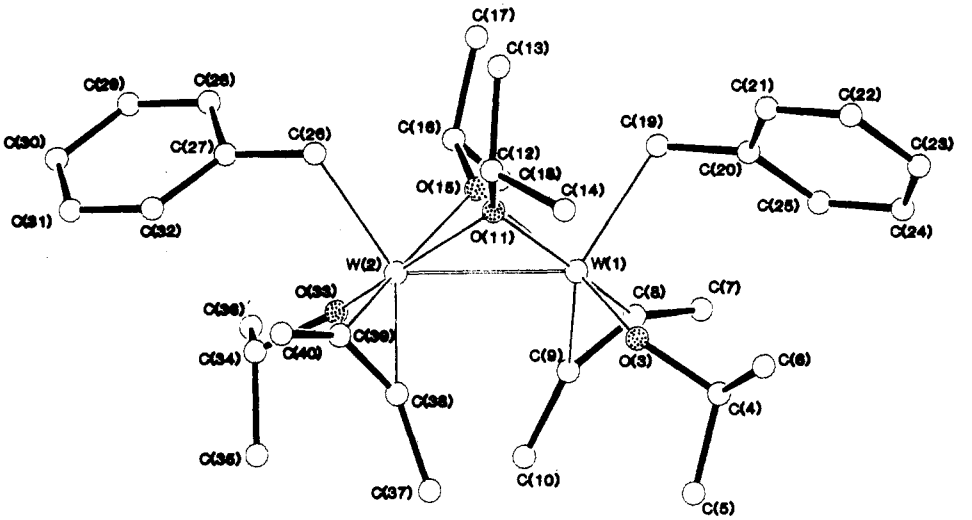

Figure 1. Ball-and-stick drawing of the $W_2(CH_2Ph)_2(MeCCMe)_2(O\text{-}i\text{-}Pr)_4$ molecule viewed perpendicular to the virtual C_2 axis.

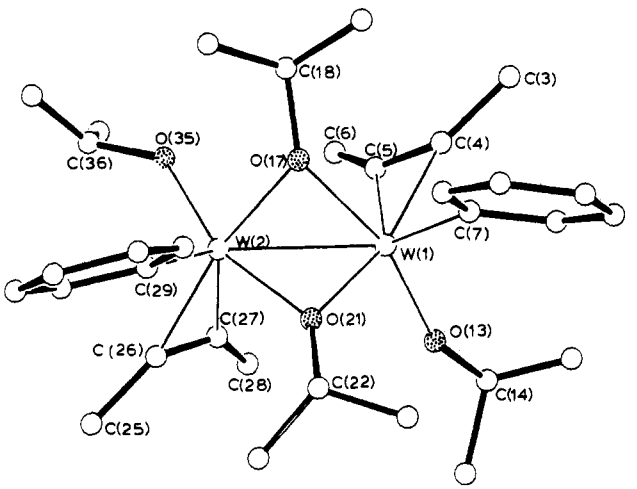

Figure 2. Ball-and-stick drawing of the $W_2(C_6H_5)_2(MeCCMe)_2(O\text{-}i\text{-}Pr)_4$ molecule viewed down the virtual C_2 axis.

also air-sensitive in solution and in the solid state. Compound **4** has been structurally characterized by single-crystal X-ray diffraction, and **4** and **5** have been spectroscopically characterized by ^1H and ^{13}C NMR and IR. Due to the thermal instability of these complexes, elemental analysis was not attempted.

1,1-$W_2Me_2(\mu\text{-MeCCMe})(O\text{-}t\text{-Bu})_4(py)$ and $W_2Me(\mu\text{-HCCH})(O\text{-}t\text{-Bu})_5(py)$. Addition of 2-butyne to pentane solutions of 1,2-$W_2Me_2(O\text{-}t\text{-Bu})_4(py)_2$ at 0 °C results in the rapid formation of 1,1-$W_2Me_2(\mu\text{-MeCCMe})(O\text{-}t\text{-Bu})_4(py)$ (**6**) according to eq 9. Reaction 9 represents the first fully characterized metal-to-metal alkyl migration at a $(W{\equiv}W)^{6+}$ center.

$$1,2\text{-}W_2Me_2(O\text{-}t\text{-Bu})_4(py)_2 + MeC{\equiv}CMe \rightarrow \underset{\mathbf{6}}{1,1\text{-}W_2Me_2(\mu\text{-MeCCMe})(O\text{-}t\text{-Bu})_4(py)} + py \quad (9)$$

Large blue crystals of **6** can be isolated in ca. 50% yield from cold pentane solutions. Compound **6** is extremely air-sensitive and thermally unstable in solution and in the solid state requiring extra care in isolation, NMR sample preparation, and X-ray crystallographic analysis. The solid-state structure of **6** is shown in Figure 5 and will be discussed in detail in the next section. Decomposition of **6** occurs above −20 °C in solution by an alkyne scission process forming $W(\equiv CMe)(O\text{-}t\text{-Bu})_3(py)_x$[20] ($x$ = 1 or 2) and other as yet unidentified organometallic products. The other "expected" decomposition product $W(\equiv CMe)Me_2(O\text{-}t\text{-Bu})(py)_x$ has not been identified in the reaction mixtures.

The reaction between 1,2-$W_2Me_2(O\text{-}t\text{-Bu})_4(py)_2$ and $HC{\equiv}CH$ produces $W_2Me(\mu\text{-HCCH})(O\text{-}t\text{-Bu})_5(py)$ (**7**) in a low yield. Compound **7** is formed from an apparent disproportionation involving intermolecular alkyl and alkoxide group transfer. ^1H and ^{13}C NMR spectra of crude reaction mixtures involving ethyne and $W_2Me_2(O\text{-}t\text{-Bu})_4(py)_2$ reveal other organometallic products that have not been isolated or unequivocally characterized thus far. The spectroscopic data for **7** are consistent with a structure similar to that seen for **6** and will be discussed in the next section.

Compounds **6** and **7** have been characterized by IR and ^1H and ^{13}C NMR spectroscopy, and compound **6** has been characterized by X-ray crystallography. Compound **7** was characterized by elemental analysis, but due to the thermal instability of **6**, elemental analysis was not attempted.

Solid-State Molecular Structures and Bonding

$W_2R_2(R'CCR'')_2(O\text{-}i\text{-Pr})_4$. Ball-and-stick drawings of the $W_2(CH_2Ph)_2(MeCCMe)_2(O\text{-}i\text{-Pr})_4$ and $W_2(C_6H_5)_2(MeCCMe)_2(O\text{-}i\text{-Pr})_4$ molecules are shown in Figures 1 and 2, respectively. The corresponding selected bond distances and angles are listed in Tables I and II, and the comparisons given in Table III emphasize the structural similarities of the two compounds. The fractional coordinates are given in Tables IV and V, respectively, and summaries of the crystal data for both compounds are given in Table VI.

The local geometry about each tungsten atom in the dinuclear compounds **2** is square-pyramidal with the alkyl or aryl ligands occupying the apical positions. The two metal fragments are fused along a common basal edge through bridging alkoxide ligands to form dinuclear units. The overall molecular geometries have virtual C_2 symmetry and contain puckered $W_2(\mu\text{-O-}i\text{-Pr})_2$ cores reminiscent of the central $Co_2(\mu\text{-CO})_2$ core in $Co_2(CO)_8$.[32] The W–W distances of 2.6684 (6) and 2.6577 (6) Å, for R = CH_2Ph and C_6H_5, respectively, are indicative of W–W single bonds (versus ca. 2.3 Å for a W≡W triple bond)[14] suggesting a net four-electron oxidation of the W_2 centers upon ligation of two alkynes. The lengthening of the C–C acetylenic bonds from 1.21 Å in free acetylene to 1.31 Å (average for the coordinated alkynes in **2**) reflects metal-to-alkyne π^* back-bonding consistent with the formal oxidation of the

(32) Sumner, G. G.; Klug, H. P.; Alexander, L. E. *Acta Crystallogr.* **1964**, *17*, 732.

Table II. Selected Bond Distances (Å) and Angles (deg) for $W_2(C_6H_5)_2(MeCCMe)_2(O\text{-}i\text{-}Pr)_4$

Bond Distances			
W(1)-W(2)	2.6577 (6)	W(2)-O(17)	2.111 (6)
W(1)-O(13)	1.850 (6)	W(2)-O(21)	2.132 (5)
W(1)-O(17)	2.209 (5)	W(2)-O(35)	1.866 (6)
W(1)-O(21)	2.066 (6)	W(2)-C(26)	2.062 (8)
W(1)-C(4)	2.054 (9)	W(2)-C(27)	2.039 (9)
W(1)-C(5)	2.050 (9)	W(2)-C(29)	2.182 (9)
W(1)-C(7)	2.165 (8)	C(4)-C(5)	1.315 (13)
		C(26)-C(27)	1.313 (13)
Bond Angles			
W(2)-W(1)-O(13)	114.86 (18)	O(21)-W(2)-C(29)	81.82 (28)
W(2)-W(1)-C(7)	125.15 (23)	O(35)-W(2)-C(29)	104.4 (3)
O(13)-W(1)-O(21)	91.68 (24)	W(1)-O(13)-C(14)	151.0 (7)
O(13)-W(1)-C(7)	104.4 (3)	W(1)-O(17)-W(2)	75.89 (18)
O(17)-W(1)-C(7)	82.18 (27)	W(1)-O(21)-W(2)	78.55 (19)
O(21)-W(1)-C(7)	92.1 (3)	W(2)-O(35)-C(36)	139.2 (6)
W(1)-W(2)-O(35)	114.76 (18)	C(3)-C(4)-C(5)	138.3 (9)
W(1)-W(2)-C(29)	124.51 (24)	C(4)-C(5)-C(6)	140.0 (9)
O(17)-W(2)-O(35)	89.15 (24)	C(25)-C(26)-C(27)	136.1 (9)
O(17)-W(2)-C(29)	91.02 (27)	C(26)-C(27)-C(28)	137.9 (9)

Table III. Comparison of Pertinent Bond Distances (Å) and Angles (deg) for Compounds $W_2R_2(MeCCMe)_2(O\text{-}i\text{-}Pr)_4$ Where R = CH_2Ph and C_6H_5

	R = CH_2Ph	R = C_6H_5
	Bond Distances[a,b]	
W-W	2.668 (1)	2.658 (1)
W-C(R)	2.21 (1)	2.17 (2)
W-O_t	1.86 (1)	1.86 (2)
W-O_b	2.15 (2)/2.07 (1)	2.17 (4)/2.09 (3)
W-C(alkyne)	2.05 (2)	2.05 (2)
C-C(alkyne)	1.31 (2)	1.31 (2)
	Bond Angles[a,b]	
C-C-C(alkyne)	136 (2)/140 (1)	137 (2)/139 (2)
W-W-C(R)	123 (1)	125 (1)
W-O_t-C	141 (4)	145 (6)

[a] Averaged where appropriate. [b] The subscripts t and b denote terminal and bridging O-*i*-Pr ligands, respectively.

W_2 centers. Furthermore, the W-C(alkyne) distances of 2.05 Å (average) are indicative of W-C multiple bonds.[33] These data are consistent with W_2^{10+} metal centers each having two metallacyclopropene moieties formed from "2 minus" alkyne ligands. The bridging alkoxide ligands asymmetrically span the W_2 centers. There are long W-O bonds trans to the terminal W-OR bonds (W-O = 2.16 Å (average)) and short W-O bonds trans to the η^2-C_2Me_2 moieties (W-O = 2.08 Å (average)). The terminal alkoxide ligands display short W-O distances (1.86 Å (average)) and large W-O-C angles (143° (average)) signifying extensive oxygen-to-metal π bonding. The W-C(alkyl or aryl) bond distances are statistically equivalent in the two molecules although a shorter W-C(aryl) bond versus a W-C(alkyl) bond might have been expected due to the differences in covalent radii of sp^2 (aryl) and sp^3 (alkyl) carbon atoms. There is *no* apparent metal-to-aryl π^* back-bonding[34] in the $W_2Ar_2(MeCCMe)_2(O\text{-}i\text{-}Pr)_4$ compounds as evidenced by (1) the small 7.5 ± 0.2 kcal mol^{-1} barrier to rotation about the W-C(C_6H_4-*p*-Me) bond in $W_2(C_6H_4\text{-}p\text{-}Me)_2(MeCCMe)_2(O\text{-}i\text{-}Pr)_4$ in solution at −120 °C and (2) the W-C(phenyl) distance of 2.17 (2) Å in the solid-state X-ray structure of $W_2(C_6H_5)_2(MeCCMe)_2(O\text{-}i\text{-}Pr)_4$ that equals the sum of the covalent radii of W(V) and sp^2 carbon indicating "σ-only" W-C(phenyl) bonds.

(33) The W-η^2-C_2 distances are comparable to those seen in $W_2(O\text{-}i\text{-}Pr)_6(\mu\text{-}C_4R_4)(\eta^2\text{-}C_2R_2)$ compounds where R = H and Me,[17] which together with the low-field chemical shifts allows the alkyne to be viewed as a 4-electron π-donor. See ref 35.

(34) Jones, W.; Feher, F. J. *Inorg. Chem.* **1984**, *23*, 2376.

Table IV. Fractional Coordinates for $W_2(CH_2Ph)_2(MeCCMe)_2(O\text{-}i\text{-}Pr)_4$

atom	10^4x	10^4y	10^4z	B_{iso}, Å^2
W(1)	7953.6 (2)	1476.2 (1)	1936.7 (2)	9
W(2)	6904.5 (2)	1527.2 (1)	3344.7 (2)	10
O(3)	7230 (4)	1933 (2)	954 (3)	16
C(4)	7537 (6)	2339 (4)	223 (4)	17
C(5)	7396 (6)	3119 (4)	394 (5)	20
C(6)	6780 (6)	2069 (4)	−582 (4)	20
C(7)	10775 (6)	1852 (4)	1921 (5)	24
C(8)	9568 (6)	1878 (4)	2056 (4)	16
C(9)	8946 (5)	2304 (3)	2448 (4)	14
C(10)	9033 (6)	2996 (4)	2922 (4)	18
O(11)	6471 (3)	972 (2)	2139 (3)	11
C(12)	5500 (5)	606 (4)	1729 (4)	16
C(13)	5684 (6)	−197 (4)	1769 (5)	20
C(14)	5167 (6)	866 (4)	805 (5)	22
O(15)	8269 (3)	896 (2)	3155 (3)	11
C(16)	9093 (6)	554 (3)	3779 (4)	17
C(17)	9141 (6)	−244 (4)	3595 (5)	22
C(18)	10215 (7)	902 (4)	3805 (5)	27
C(19)	8699 (5)	487 (4)	1473 (4)	14
C(20)	8659 (6)	492 (4)	504 (4)	19
C(21)	7859 (6)	102 (4)	−37 (5)	22
C(22)	7820 (6)	110 (4)	−935 (5)	23
C(23)	8570 (6)	516 (5)	−1321 (5)	24
C(24)	9427 (6)	894 (4)	100 (5)	20
C(25)	9374 (6)	903 (4)	−798 (5)	24
C(26)	6085 (6)	587 (4)	3853 (4)	16
C(27)	6165 (5)	639 (3)	4812 (4)	15
C(28)	6985 (6)	280 (4)	5372 (5)	21
C(29)	7083 (6)	338 (5)	6254 (5)	27
C(30)	6344 (7)	764 (4)	6647 (5)	26
C(31)	5506 (6)	1122 (4)	6116 (5)	21
C(32)	5411 (6)	1063 (4)	5217 (4)	19
O(33)	7742 (4)	1901 (2)	4337 (3)	16
C(34)	7694 (6)	2244 (4)	5150 (4)	18
C(35)	7455 (6)	3038 (4)	4994 (5)	22
C(36)	8806 (8)	2111 (4)	5711 (5)	33
C(33)	6017 (6)	3159 (4)	2518 (5)	23
C(38)	6017 (5)	2422 (3)	2891 (4)	13
C(39)	5321 (6)	1960 (4)	3185 (4)	17
C(40)	4094 (7)	1914 (5)	3230 (5)	30

The fused square-pyramidal geometry of the $W_2R_2(R'CCR'')_2(O\text{-}i\text{-}Pr)_4$ compounds (**2**) is unique among dinuclear tungsten and molybdenum complexes[14] containing five-coordinate metal atoms and M-M bond orders of 0→2. The local geometry about each metal atom results from optimization of metal-ligand π bonding, and the puckering of the $M_2(\mu\text{-}O\text{-}i\text{-}Pr)_2$ core presumably occurs to optimize metal-metal bonding. The metal-ligand and metal-metal interactions can easily be understood, qualitatively, by first examining the π interactions in the square-pyramidal d^3 ML_5 fragment followed by bringing two such fragments together to form the observed molecular structures.

A schematic drawing of the ligand geometry about each metal center of **2** is depicted by III. The alignment of the

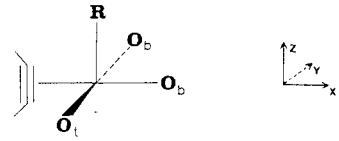

III, O = alkoxide, R = alkyl or aryl

coordinate system in the description of this fragment is particularly important as metal-to-alkyne π donation hinges upon the correct orientation of the metal d orbitals with respect to the alkyne π^* orbitals. The alkyl or aryl ligand (R) and two bridging alkoxide ligands (O_b) are "σ only" donors and are not involved in π bonding in the ML_5 fragment. The three important metal-ligand π interactions are as follows: (1) The filled acetylenic C-C π-bonding orbital perpendicular to the metal-alkyne vector

Table V. Fractional Coordinates for $W_2(C_6H_5)_2(MeCCMe)_2(O\text{-}i\text{-}Pr)_4$

atom	10^4x	10^4y	10^4z	B_{iso}, Å^2
W(1)	7543.9 (3)	1599.0 (2)	3138.1 (2)	12
W(2)	8581.1 (3)	1105.6 (2)	1884.4 (2)	11
C(3)	8409 (8)	2988 (5)	4598 (7)	23
C(4)	8413 (8)	2335 (5)	4063 (6)	18
C(5)	9164 (8)	1859 (5)	3984 (6)	16
C(6)	10401 (8)	1650 (5)	4427 (7)	21
C(7)	6115 (7)	2328 (5)	2829 (6)	15
C(8)	5578 (8)	2481 (5)	3550 (6)	17
C(9)	4525 (8)	2857 (5)	3367 (7)	24
C(10)	4031 (9)	3110 (5)	2472 (7)	25
C(11)	4548 (9)	2972 (5)	1761 (6)	23
C(12)	5561 (7)	2583 (5)	1928 (6)	16
O(13)	7106 (5)	947 (3)	3888 (4)	17
C(14)	7152 (9)	665 (5)	4800 (7)	58
C(15)	6677 (9)	1073 (5)	5378 (7)	52
C(16)	6760 (9)	−72 (5)	4673 (7)	53
O(17)	7960 (5)	2114 (3)	1931 (4)	13
C(18)	8652 (8)	2718 (4)	1885 (6)	17
C(19)	8083 (9)	3359 (5)	2131 (7)	24
C(20)	8817 (8)	2786 (4)	897 (7)	20
O(21)	6801 (5)	1045 (3)	1927 (4)	14
C(22)	5711 (8)	721 (5)	1452 (7)	26
C(23)	4812 (10)	796 (6)	1991 (9)	38
C(24)	5905 (10)	−4 (6)	1215 (10)	44
C(25)	8755 (9)	−592 (5)	1299 (7)	25
C(26)	8792 (7)	62 (4)	1811 (7)	16
C(27)	9038 (8)	253 (5)	2700 (7)	21
C(28)	9537 (10)	−58 (5)	3654 (7)	31
C(29)	7763 (8)	1049 (4)	366 (6)	16
C(30)	8217 (9)	658 (5)	−248 (6)	20
C(31)	7749 (9)	680 (5)	−1212 (7)	24
C(32)	6793 (9)	1096 (5)	−1619 (6)	22
C(33)	6336 (8)	1504 (5)	−1032 (7)	23
C(34)	6830 (8)	1486 (5)	−61 (6)	17
O(35)	10073 (5)	1457 (3)	1983 (4)	17
C(36)	11175 (8)	1236 (5)	1867 (8)	27
C(37)	12062 (17)	1129 (18)	2692 (14)	152
C(38)	11430 (15)	1506 (17)	1113 (14)	150

(π^B) π donates into the empty metal d_{xy} orbital as schematically shown by IV. The ^{13}C NMR chemical shifts of

IV

the acetylenic carbons of **2** (δ 202 (average)) are diagnostic of four-electron-donor alkyne ligands[35] ($2\sigma + 2\pi$) indicating that this interaction is quite strong. (2) The terminal alkoxide ligand π donates into the empty metal d_{yz} orbital as shown in V. The short W–O bond distances (1.86 Å

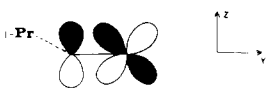

V

(average)) are indicative of significant alkoxide π donation.[14] (3) The empty acetylenic C–C π-antibonding orbital parallel to the metal–alkyne vector ($\pi_\parallel$*) π accepts from the filled metal d_{xz} orbital in a back-bonding interaction as shown in VI. This interaction is responsible for the

VI

lengthening of the W–W bond from ca. 2.3 to 2.7 Å

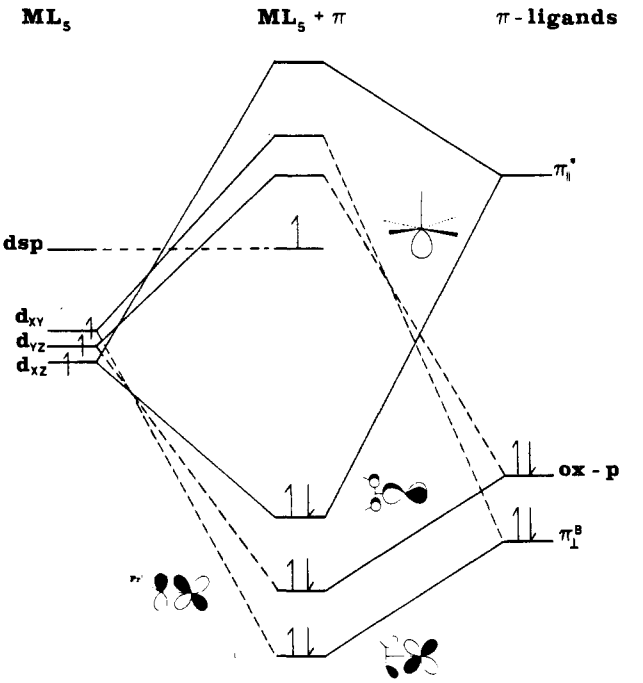

Figure 3. Qualitative molecular orbital interaction diagram illustrating the effects of π bonding in the ML_5 fragment of $W_2R_2(R'CCR'')_2(O\text{-}i\text{-}Pr)_4$ compounds (**2**).

(four-electron oxidation of the W_2 center) and the lengthening of the C–C acetylenic bond from 1.21 to 1.31 Å ($2e^-$ reduction of *each* alkyne). Acetylenic π acceptance dominates metal–ligand π bonding in other tungsten–alkyne compounds[36] containing π-donor ancillary ligands and appears to be equally strong in the present compounds. However, the metal-based electrons in the M_2X_6 compounds are ca. 0.5 eV lower in energy for Mo relative to W.[8] The Mo d electrons are therefore energetically less accessible to the alkyne π* orbitals and metal-to-alkyne π back-bonding is significantly weakened. Presumably, this change in orbital energy diminishes Mo-to-alkyne π back-bonding and precludes the isolation of 1,2-Mo_2R_2-$(R'CCR'')_2(O\text{-}i\text{-}Pr)_4$ compounds. The relative orbital energies of the filled C–C π orbitals are also important in contributing to the alkyne–metal bond and is evidenced by the formation of complexes **2** where R′ = R″ = Me and Et but not for R′ and R″ = H or Ph.

The orbital splittings of the remnant t_{2g} set in the d^3 ML_5 fragment of **2** are illustrated in the qualitative molecular orbital diagram shown in Figure 3. The three pertinent metal–ligand π interactions just described occur *without orbital competition* at the metal center. The formation of the dinuclear compound **2** is accomplished by joining two of the ML_5 units (III) via superpositioning the O_b groups on each fragment. By puckering the W_2-$(\mu\text{-}O_b)_2$ core, the "dsp" hybrid orbitals (VII) on each metal atom can interact to form a "bent" W–W σ bond (VIII)

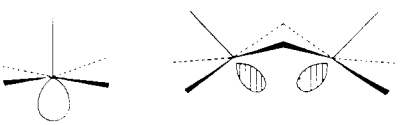

VII VIII

as shown. Because of the low overall molecular symmetry (C_2), orbital mixing can occur to increase M–M σ overlap. Preliminary Fenske–Hall molecular orbital calculations[37]

(35) Templeton, J. L.; Ward, B. C. *J. Am. Chem. Soc.* **1980**, *102*, 3288.

(36) Hoffmann, R.; Templeton, J. L. *Inorg. Chem.* **1983**, *21*, 466.
(37) Chisholm, M. H.; Eichhorn, B. W., unpublished results.

Table VI. Summaries of Crystallographic Data[a]

	A	B	C	D
empirical formula	$W_2C_{34}H_{54}O_4$	$W_2C_{32}H_{50}O_4$	$W_2C_{28}H_{60}O_4$	$W_2C_{27}O_4NH_{53}$
color of cryst	black	red-orange	yellow-brown	red-black
cryst dimens (mm)	0.14 × 0.14 × 0.17	0.04 × 0.048 × 0.064	0.10 × 0.12 × 0.12	0.08 × 0.08 × 0.12
space group	$P2_1/n$	$P2_1/n$	$P\bar{1}$	$P2_1/c$
cell dimens				
temp (0 °C)	−159	−159	−155	−162
a (Å)	11.999 (2)	11.843 (2)	9.947 (2)	9.468 (3)
b (Å)	18.650 (4)	19.543 (4)	10.481 (2)	35.968 (16)
c (Å)	15.522 (3)	14.699 (2)	9.457 (2)	10.176 (3)
α (deg)			93.40 (1)	
β (deg)	97.84 (1)	105.70 (1)	108.07 (1)	113.68 (2)
γ (deg)			107.66 (1)	
Z (molecules/cell)	4	4	1	4
V (Å^3)	3440.93	3278.08	880.31	3173.49
d(calcd), (g/cm^3)	1.727	2.756	1.563	1.724
wavelength (Å)	0.710 69	0.710 69	0.710 69	0.710 69
mol wt	894.50	866.44	828.48	823.42
linear abs coeff (cm^{-1})	68.573	71.950	66.940	74.293
detector to sample dist (cm)	22.5	22.5	22.5	22.5
sample to souuce dist (cm)	23.5	23.5	23.5	23.5
av ω scan width at half-height	.25	0.25	0.25	0.25
scan speed (deg/min)	4.0	6.0	4.0	4.0
scan width (deg + dispersn)	2.0	1.6	2.0	2.0
individual bkgd (s)	8	8	6	6
aperture size (mm)	3.0 × 4.0	3.0 × 4.0	3.0 × 4.0	3.0 × 4.0
2θ range (deg)	6–45	6–45	6–45	6–45
total no. of reflctns collected	4757	7572	3750	4351
no. of unique intensities	4511	4304	3750	4156
no. of $F > 0.0$		4087		
no. of $F > 3.0\sigma(F)$	3874	3803	2944	3405
$R(F)$	0.0254	0.0335	0.0357	0.0514
$R_w(F)$	0.0301	0.0342	0.0363	0.0517
goodness of fit for the last cycle	0.703	0.961	1.173	1.173
max Δ/σ for the last cycle	0.05	0.05	0.05	0.05

[a] A, $W_2(CH_2Ph)_2(MeCCMe)_2(O\text{-}i\text{-}Pr)_4$; B, $W_2(C_6H_5)_2(MeCCMe)_2(O\text{-}i\text{-}Pr)_4$; C, $[W(\equiv CEt)(CH_2\text{-}t\text{-}Bu)(O\text{-}i\text{-}Pr)_2]_2$; D, 1,1-$W_2Me_2(\mu\text{-}C_2Me_2)(O\text{-}t\text{-}Bu)_4(py)$.

indicated that extensive orbital mixing does occur, and the resultant M–M σ bond is virtually linear (i.e. electron density resides along the M–M axis). Had the ligands adopted a trigonal-bipyramidal geometry (which is most commonly observed[14] for similar dinulcear W and Mo compounds), several metal–ligand orbital conflicts would exist, weakening the metal–ligand bonds. However, the dinuclear compounds based on fused trigonal-bipyramidal fragments, e.g. as in $Mo_2(O\text{-}i\text{-}Pr)_8$[38] and $Mo_2(\mu\text{-}S)_2(S\text{-}t\text{-}Bu)_4(HNMe_2)_2$,[39] presumably have better M–M overlap compared to the fused square-pyramidal geometries observed in the present compounds **2**. Even the non M–M bonded compounds $Mo_2(\mu\text{-}O\text{-}i\text{-}Pr)_2(O\text{-}i\text{-}Pr)_4(NO)_2$[40] and $W_2(\equiv CMe)_2(\mu\text{-}O\text{-}t\text{-}Bu)_2(O\text{-}t\text{-}Bu)_4$[41] adopt fused (axial–equatorial) tbp geometries. These data suggest that the observed molecular structures of **2** reflect optimization of metal–ligand bonding at the expense of metal–metal bonding. This phenomenon has been observed in other dimetal compounds.[42]

Rotation of the alkyne ligand by 90° about the metal–alkyne vector in III inverts the donor–acceptor roles of the tungsten d_{xz} and d_{xy} orbitals with respect to metal–alkyne π bonding (IV, VI). The qualitative molecular orbital diagram, however, remains essentially unchanged, suggesting that the barrier to alkyne rotation should be small and mostly steric in origin. Spectroscopically, alkyne rotation has been monitored and the rotational barriers ($\Delta G^{\ddagger}_{rot,}$) were determined to be 9.6 kcal mol^{-1} (average). These values are approximately 50% smaller than those observed for other alkyne complexes in which electronic barriers to alkyne rotation exist at a d^2 metal center.[43,44]

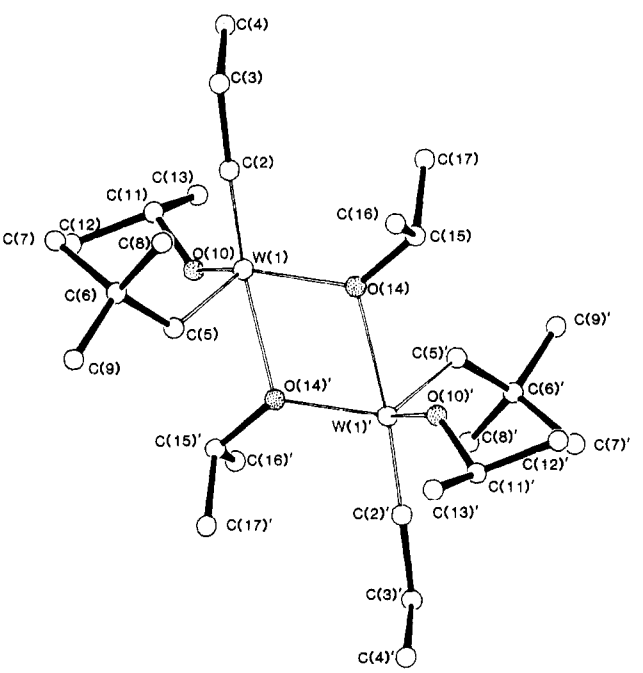

Figure 4. Ball-and-stick drawing of the $[W(\equiv CEt)(CH_2\text{-}t\text{-}Bu)(O\text{-}i\text{-}Pr)_2]_2$ molecule (**4**).

(38) Chisholm, M. H.; Cotton, F. A.; Extine, M. W.; Reichert, W. W. *Inorg. Chem.* **1978**, *17*, 2944.
(39) Chisholm, M. H.; Corning, J. F.; Huffman, J. C. *Inorg. Chem.* **1982**, *21*, 286.
(40) Chisholm, M. H.; Cotton, F. A.; Extine, M. W.; Kelly, R. L. *J. Am. Chem. Soc.* **1978**, *100*, 3354.
(41) Chisholm, M. H.; Hoffman, D. M.; Huffman, J. C. *Inorg. Chem.* **1983**, *22*, 2903.
(42) (a) Teo, B. K.; Hall, M. B.; Fenske, R. F.; Dahl, L. F. *Inorg. Chem.* **1975**, *14*, 3103. (b) Norman, J. G., Jr.; Osborne, J. H. *Inorg. Chem.* **1982**, *21*, 3241.

Table VII. Selected Bond Distances (Å) and Angles (deg) for $[W(\equiv CEt)(CH_2\text{-}t\text{-}Bu)(O\text{-}i\text{-}Pr)_2]_2$

Bond Distances			
W(1)–W(1)′	3.514 (1)	W(1)–C(2)	1.765 (7)
W(1)–O(10)	1.882 (5)	W(1)–C(5)	2.105 (7)
W(1)–O(14)	1.961 (5)	C(2)–C(3)	1.503 (10)
W(1)–O(14)′	2.365 (5)		

Bond Angles			
O(10)–W(1)–O(14)	80.20 (20)	O(14)–W(1)–C(5)	112.25 (24)
O(10)–W(1)–C(2)	102.2 (3)	C(2)–W(1)–C(5)	99.0 (3)
O(10)–W(1)–C(5)	110.78 (26)	W(1)–O(10)–C(11)	134.6 (5)
O(14)–W(1)–O(14)′	71.74 (20)	W(1)–O(14)–W(1)′	108.26 (20)
O(14)–W(1)–C(2)	103.10 (27)	W(1)–C(2)–C(3)	178.0 (6)

Table VIII. Fractional Coordinates for $[W(\equiv CEt)(CH_2\text{-}t\text{-}Bu)(O\text{-}i\text{-}Pr)_2]_2$

atom	10^4x	10^4y	10^4z	B_{iso}, Å^2
W(1)	1569.5 (3)	1476.4 (3)	852.3 (3)	14
C(2)	3267 (8)	2139 (7)	2403 (9)	20
C(3)	4728 (9)	2662 (8)	3707 (9)	26
C(4)	6044 (9)	2502 (9)	3302 (10)	32
C(5)	444 (8)	2750 (7)	1363 (8)	19
C(6)	1044 (9)	4031 (8)	2568 (8)	22
C(7)	2416 (9)	5073 (8)	2388 (9)	26
C(8)	1487 (11)	3649 (9)	4146 (9)	29
C(9)	−164 (10)	4691 (8)	2429 (10)	29
O(10)	2203 (6)	1947 (5)	−784 (6)	22
C(11)	3621 (9)	2635 (10)	−937 (10)	33
C(12)	3463 (13)	3842 (16)	−1707 (18)	72
C(13)	4045 (18)	1712 (20)	−1736 (29)	122
O(14)	715 (5)	−386 (5)	1170 (5)	17
C(15)	1200 (8)	−1091 (7)	2413 (8)	20
C(16)	1121 (10)	−418 (9)	3835 (9)	31
C(17)	2732 (9)	−1165 (8)	2575 (10)	27

$[W(\equiv CEt)(CH_2\text{-}t\text{-}Bu)(O\text{-}i\text{-}Pr)_2]_2$ and $[W(\equiv CEt)(CH_2\text{-}t\text{-}Bu)(O\text{-}i\text{-}Pr)_2(py)]_2$. A ball-and-stick drawing of the $[W(\equiv CEt)(CH_2\text{-}t\text{-}Bu)(O\text{-}i\text{-}Pr)_2]_2$ molecule (**4**) is shown in Figure 4, and the corresponding selected bond distances and angles are listed in Table VII. Fractional coordinates are given in Table VIII, and a summary of the crystal data is given in Table VI. The tungsten atoms are in distorted trigonal-bipyramidal coordination environments with two O-*i*-Pr ligands and a CH_2-*t*-Bu ligand occupying equatorial positions. The equatorial W–O distance of 1.88 (1) Å indicates significant oxygen-to-metal π bonding.[14] The propylidyne moiety is axially coordinated and displays a trypical W≡C distance of 1.76 (2) Å.[45] The two trigonal-bipyramidal fragments are joined along a common axial–equatorial edge by virtue of weak, dative O-*i*-Pr bonds [(W(1)–O(14)′ = 2.36 (2) Å). The skeletal geometry of **4** is very similar to that of $[W(\equiv CMe)(O\text{-}t\text{-}Bu)_3]_2$.[41]

In the solid state, $W(\equiv CEt)(CH_2\text{-}t\text{-}Bu)(O\text{-}i\text{-}Pr)_2(py)$ is presumably dimeric with an edge-shared bioctahedral geometry similar to that of $[W(\equiv CEt)(O\text{-}i\text{-}Pr)_3(HNMe_2)]_2$.[29] The proposed structure of **5** is depicted by IX. Because of the high trans influence of alkyl ligands, the CH_2-*t*-Bu groups are assigned to axial positions trans to the weakly bound py ligands.

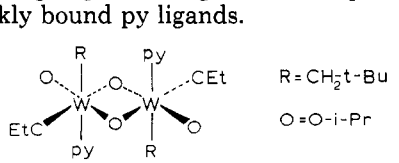

IX

Table IX. Selected Bond Distances (Å) and Angles (deg) for $1,1\text{-}W_2Me_2(\mu\text{-}C_2Me_2)(O\text{-}t\text{-}Bu)_4(py)$

Bond Distances			
W(1)–W(2)	2.6223 (12)	W(2)–O(23)	2.064 (9)
W(1)–O(7)	1.902 (9)	W(2)–O(28)	1.873 (11)
W(1)–O(12)	1.917 (9)	W(2)–C(4)	2.065 (17)
W(1)–O(23)	2.046 (10)	W(2)–C(5)	2.222 (15)
W(1)–N(17)	2.216 (12)	W(2)–C(33)	2.233 (16)
W(1)–C(4)	2.120 (14)	W(2)–C(34)	2.162 (16)
W(1)–C(5)	2.054 (16)	C(4)–C(5)	1.412 (19)

Bond Angles			
W(2)–W(1)–O(7)	106.6 (3)	C(4)–W(2)–C(5)	38.2 (5)
W(2)–W(1)–O(12)	120.8 (3)	C(4)–W(2)–C(34)	121.3 (6)
W(2)–W(1)–N(17)	137.4 (3)	C(5)–W(2)–C(34)	84.7 (6)
W(1)–W(2)–O(28)	120.9 (3)	C(33)–W(2)–C(34)	81.0 (6)
W(1)–W(2)–C(33)	132.4 (4)	W(1)–O(7)–C(8)	146.4 (9)
W(1)–W(2)–C(34)	107.4 (4)	W(1)–O(12)–C(13)	153.9 (10)
O(23)–W(2)–C(33)	171.4 (5)	W(1)–O(23)–W(2)	79.3 (3)
O(28)–W(2)–C(4)	114.5 (5)	W(1)–O(23)–C(24)	138.1 (9)
O(28)–W(2)–C(5)	152.8 (5)	W(2)–O(23)–C(24)	142.7 (9)
O(28)–W(2)–C(33)	89.1 (6)	W(2)–O(28)–C(29)	158.7 (11)
O(28)–W(2)–C(34)	121.2 (6)	C(3)–C(4)–C(5)	130.0 (15)
		C(4)–C(5)–C(6)	134.9 (14)

Table X. Fractional Coordinates for $1,1\text{-}W_2Me_2(\mu\text{-}C_2Me_2)(O\text{-}t\text{-}Bu)_4(py)$

atom	10^4x	10^4y	10^4z	B_{iso}, Å^2
W(1)	5436 (1)	1139.2 (2)	8445 (1)	12
W(2)	2982 (1)	1456.7 (2)	8532 (1)	14
C(3)	1913 (18)	771 (5)	6203 (16)	25
C(4)	3091 (16)	975 (5)	7473 (15)	20
C(5)	3792 (18)	871 (4)	8933 (14)	16
C(6)	3508 (20)	577 (5)	9825 (18)	28
O(7)	5677 (11)	1337 (3)	6814 (9)	18
C(8)	5040 (18)	1364 (4)	5261 (14)	18
C(9)	4680 (19)	986 (4)	4560 (15)	19
C(10)	6330 (21)	1537 (5)	4947 (16)	28
C(11)	3601 (19)	1608 (5)	4805 (14)	25
O(12)	7212 (11)	1040 (3)	10175 (9)	21
C(13)	8148 (19)	812 (5)	11398 (16)	21
C(14)	7880 (26)	406 (6)	11017 (19)	44
C(15)	7655 (20)	897 (6)	12623 (17)	33
C(16)	9783 (20)	920 (6)	11780 (18)	37
N(17)	6023 (15)	606 (3)	7695 (12)	18
C(18)	7365 (18)	603 (4)	7529 (17)	21
C(19)	7929 (20)	296 (5)	7129 (17)	28
C(20)	7083 (23)	−27 (5)	6866 (18)	33
C(21)	5726 (20)	−34 (5)	7032 (16)	26
C(22)	5259 (0)	286 (4)	7463 (15)	22
O(23)	5201 (10)	1657 (3)	9168 (9)	13
C(24)	6134 (17)	1972 (4)	9763 (15)	18
C(25)	6271 (37)	2198 (9)	8537 (34)	22 (6)
C(26)	7814 (46)	1850 (11)	10810 (42)	38 (8)
C(27)	5343 (41)	2211 (10)	10475 (38)	30 (7)
O(28)	2029 (12)	1857 (3)	7325 (11)	25
C(29)	817 (19)	2110 (5)	6484 (17)	27
C(30)	−22 (22)	1937 (5)	4987 (18)	31
C(31)	9735 (22)	2164 (6)	7227 (18)	39
C(32)	1630 (24)	2476 (5)	6375 (22)	41
C(33)	656 (18)	1238 (5)	8196 (16)	23
C(34)	3234 (18)	1446 (5)	10740 (17)	26
C(25)′	7332 (50)	1984 (13)	9141 (47)	45 (9)
C(26)′	6994 (52)	1885 (13)	11363 (47)	46 (9)
C(27)′	5123 (52)	2322 (13)	9301 (48)	47 (9)

$1,1\text{-}W_2Me_2(\mu\text{-}MeCCMe)(O\text{-}t\text{-}Bu)_4(py)$ and $W_2Me(\mu\text{-}C_2H_2)(O\text{-}t\text{-}Bu)_5(py)$. A ball-and-stick drawing of the $1,1\text{-}W_2Me_2(\mu\text{-}MeCCMe)(O\text{-}t\text{-}Bu)_4(py)$ molecule (**6**) is shown in Figure 5, and the corresponding selected bond distances and angles are listed in Table IX. The fractional coordinates are given in Table X, and a summary of the crystal data is given in Table VI.

Compound **6** has C_1 symmetry and a slightly skewed alkyne bridge, but the skeletal geometry, W–W distance, and C–C(alkyne) distance are remarkably similar to that of the $W_2(\mu\text{-}HCCH)(O\text{-}t\text{-}Bu)_6(py)$ molecule.[46] The

(43) Templeton, J. L.; Winston, P. B.; Ward, B. C. *J. Am. Chem. Soc.* **1981**, *103*, 7713.
(44) Morrow, J. R.; Tonker, T. L.; Templeton, J. L. *Organometallics* **1985**, *4*, 745.
(45) E.g. as seen in $[(t\text{-}BuO)_3W{\equiv}CMe]_2$, ref 41, and in $(t\text{-}BuO)_3W{\equiv}CPh$, see: Cotton, F. A.; Schwotzer, W.; Shamshoum, E. W. *Organometallics* **1984**, *3*, 1770, and $[W(O\text{-}i\text{-}Pr)_3(\equiv CEt)(HNMe_2)_2$, see ref 29.

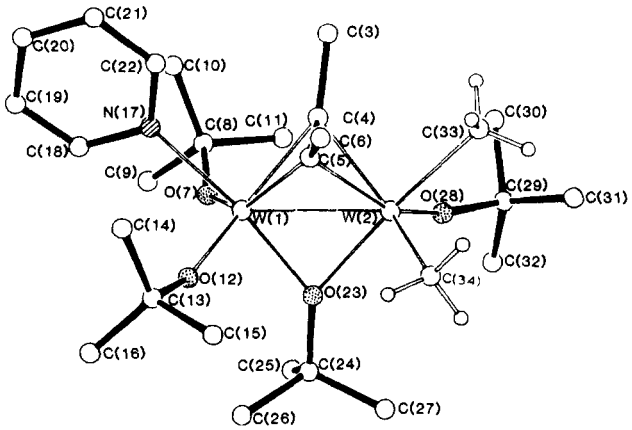

Figure 5. Ball-and-stick drawing of the 1,1-$W_2Me_2(\mu\text{-}C_2Me_2)$-(O-*t*-Bu)$_4$(py) molecule (**6**).

bonding in similar $M_2X_6(\mu\text{-RCCR})$ compounds has been discussed in detail elsewhere;[47,48] however, the following points are worthy of note. (1) The local geometry about W(2) is trigonal-bipyramidal, depicted by X, with the

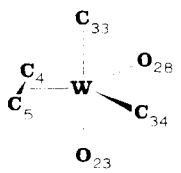

X

alkyne ligand (C(4)–C(5)) occupying a single equatorial site. The terminal O-*t*-Bu ligand (O(28)) also assumes an equatorial position to maximize oxygen-to-metal π bonding. The methyl ligands are therefore forced into one axial (C(33)) and one equatorial (C(34)) position which produces C_1 molecular symmetry. The more symmetrical equatorial–equatorial arrangement of Me groups with an axial O-*t*-Bu group (O(28)) would result in higher molecular symmetry (C_s) but weaker alkoxide π bonding. (2) The bond angles in the equatorial plane of W(1), depicted by XI, display typical angles β and δ, but α and γ decreased

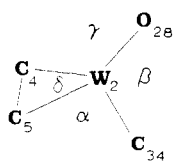

XI

and increased, respectively, when compared to other compounds of this structural type.[46] These distortions apparently occur to accommodate the sterically demanding O-*t*-Bu ligand at the expense of the small Me group. The observed geometry leaves O(28) transoid to C(5) of the alkyne, thus lengthening the W(1)–C(5) bond (2.222 (15) Å) relative to the W(1)–C(4) bond (2.065 (17) Å). It is this ground-state steric effect that causes the skewing of the alkyne ligand (6° off a 90° angle from the W–W vector) and not an electronic factor as has been seen to cause asymmetries in certain bridging alkyne complexes,[49] e.g.

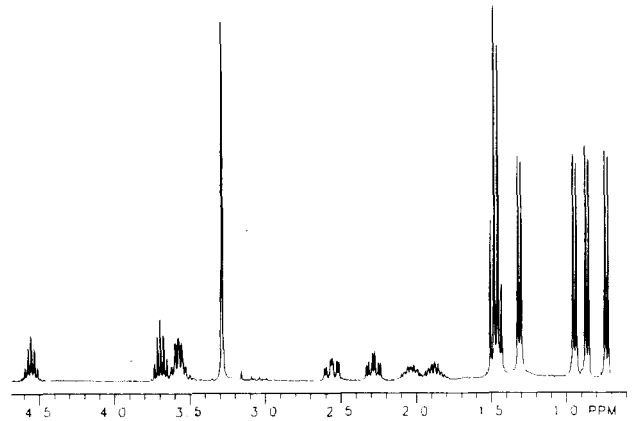

Figure 6. ^{1}H NMR spectrum of 1,2-$W_2(n\text{-Pr})_2$(MeCCEt)$_2$(O-*i*-Pr)$_4$ (**2**, R = *n*-Pr, R′ = Me, R″ = Et), recorded at 22 °C and 300 MHz in benzene-d_6 solvent.

$W_2Cl_4(NMe_2)_2(\mu\text{-}C_2Me_2)(py)_2$.[50]

The ^{1}H and ^{13}C NMR data for $W_2Me(\mu\text{-HCCH})$(O-*t*-Bu)$_5$(py) (**7**) are consistent with a symmetrically bridging alkyne complex containing a mirror plane of symmetry. The proposed structure is shown below by XII. The skeletal geometry is a perturbation of the solid-state structure of 1,1-$W_2Me_2(\mu\text{-MeCCMe})$(O-*t*-Bu)$_4$(py) (**6**) in which the equatorial Me ligand is replaced by an O-*t*-Bu group.

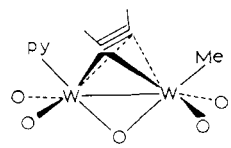

XII, O = O-*t*-Bu

Spectroscopic Studies

The room-temperature ^{1}H and ^{13}C{^{1}H} NMR data for all compounds just described are given in Table XI. The IR data are located in the Experimental Section, and the electronic absorption data are listed in Table XIII.

1,2-W_2R_2(R′CCR″)$_2$(O-*i*-Pr)$_4$ (2) and 1,2-W_2(C_6H_4-*p*-Me)$_2$(MeCCMe)$_2$(O-*t*-Bu)$_4$ (2′). The ^{1}H NMR spectrum of 1,2-$W_2(n\text{-Pr})_2$(MeCCEt)$_2$(O-*t*-Pr)$_4$ (**2**, R = *n*-Pr, R′ = Me, R″ = Et) is shown in Figure 6 as a representative of all compounds **2**. The low-temperature-limiting ^{1}H and ^{13}C NMR data for these compounds are consistent with the solid-state molecular structures previously described. At room temperature, however, the alkyne ligands are rotating rapidly on the NMR time scale and time-averaged resonances are observed for the alkyl substituents on the alkyne ligands (where R′ = R″ = Me or Et). The stacked-plot variable-temperature ^{1}H NMR spectra of 1,2-W_2(CH_2Ph)$_2$(MeCCMe)$_2$(O-*i*-Pr)$_4$ (**2**, R = CH_2Ph, R′ = R″ = Me) are shown in Figure 7 and are indicative of this fluxional process.

The α-H atoms on the alkyl ligands **2** (R = CH_2SiMe_3, CH_2Ph, Me) typically display tungsten–hydrogen couplings ($^2J_{^{183}W-^1H}$, 14% satellite intensity) of ca. 8 Hz. The α-carbon atoms of compounds **2** show tungsten–carbon couplings ($^1J_{^{183}W-^{13}C}$, 14% satellite intensity) of ca. 73 Hz (average) when R = alkyl and 101 Hz (average) when R = aryl. The α-carbon atoms of the (trimethylsilyl)methyl analogues of **2** (R = CH_2SiMe_3, R′ = R″ = Me or Et) have additional silicon–carbon couplings ($^1J_{^{29}Si-^{13}C}$, 5% satellite

(46) Chisholm, M. H.; Folting, K.; Hoffman, D. M.; Huffman, J. C. *J. Am. Chem. Soc.* **1984**, *106*, 6794.
(47) Chisholm, M. H.; Clark, D. L.; Conroy, B. K. *Polyhedron* **1988**, *7*, 903.
(48) Hoffman, D. M.; Hoffmann, R.; Fisel, C. R. *J. Am. Chem. Soc.* **1982**, *104*, 3858.
(49) Calhorda, M. J.; Hoffmann, R. *Organometallics* **1986**, *5*, 2181.
(50) Ahmed, K. J.; Chisholm, M. H.; Folting, K.; Huffman, J. C. *Organometallics* **1986**, *5*, 2171.

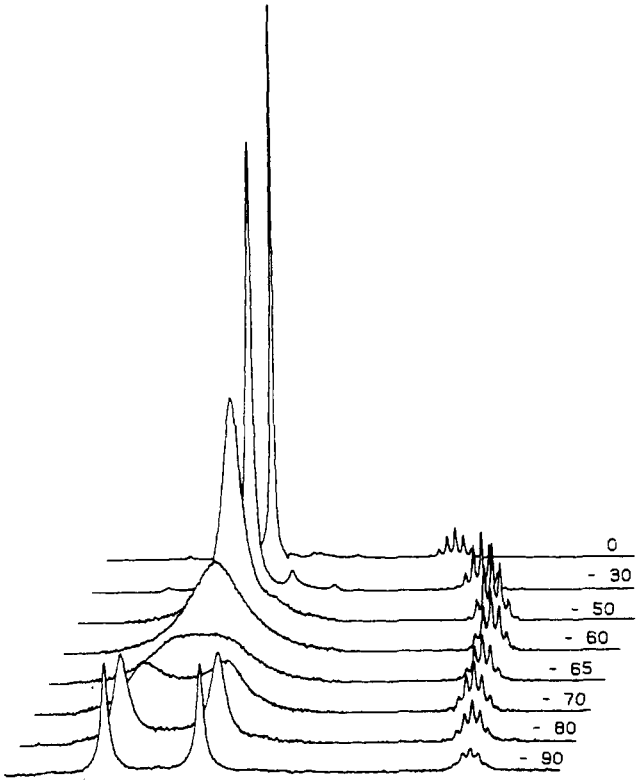

Figure 7. A stacked plot of the variable-temperature ^1H NMR spectra of 1,2-$W_2(CH_2Ph)_2(MeCCMe)_2(O\text{-}i\text{-}Pr)_4$ recorded at 360 MHz in toluene-d_8 solvent. The region shown contains the methyl resonances of the MeCCMe ligand and one of the O-*i*-Pr methine septets. The temperatures listed are in degrees centigrade, and each successive spectrum is offset ca. 0.05 ppm to the right.

intensity) of 35 Hz. The α-carbon atoms of the terminal O-*i*-Pr ligands also display tungsten coupling ($^2J_{^{183}W-^{13}C}$, 14% satellite intensity) of ca. 10 Hz whereas the bridging O-*i*-Pr ligands have $^2J_{^{183}W-^{13}C}$ couplings of less than 4 Hz (unobservable by routine methods). This phenomenon has become a useful tool for differentiating terminal from bridging alkoxide ligands on polynuclear tungsten alkoxide complexes.[51] The acetylenic carbons of the alkyne ligands have time-averaged ^{13}C NMR chemical shifts of 200–205 ppm at room temperature with $^1J_{^{183}W-^{13}C}$ values of ca. 40 Hz. At low temperatures (−40 °C), alkyne rotation is frozen out and two resonances are observed for the inequivalent acetylenic carbons.

The barriers to alkyne rotation have been monitored by ^1H NMR spectroscopy in toluene-d_8 for the symmetrical alkyne adducts (R′ = R″ = Me or Et) and the corresponding free energies of activation ($\Delta G^{\ddagger}$) calculated (Table XII). The $\Delta G^{\ddagger}$ values for all compounds **2** are ca. 9.6 kcal mol^{-1} (average) whereas $W_2(C_6H_4\text{-}p\text{-}Me)_2(MeCCMe)_2(O\text{-}t\text{-}Bu)_4$ (**2′**) has a $\Delta G^{\ddagger}$ of 14.4 ± 0.2 kcal mol^{-1}. The rotational barriers are surprisingly insensitive to the steric and electronic properties of R, R′, and R″ but exceedingly dependent upon the steric constraints of the alkoxide ligands. The barrier to rotation about the W–Ar bond ($\Delta G^{\ddagger}$) in 1,2-$W_2(C_6H_4\text{-}p\text{-}Me)_2(MeCCMe)_2(O\text{-}i\text{-}Pr)_4$ was monitored by ^1H NMR and calculated to be 7.5 ± 0.3 kcal mol^{-1} ($T_{coal.}$ = −120 °C) in $(CD_3)_2O$ solutions. No other fluxional processes were observed for compounds **2** from −130 to +60 °C.

The IR data of compounds **2** are given in the Experimental Section. No W–C(alkyl) or C–C(alkyne) stretching

(51) Allerhand, A.; Chisholm, M. H.; Hampden-Smith, M.; Maples, S., unpublished results.

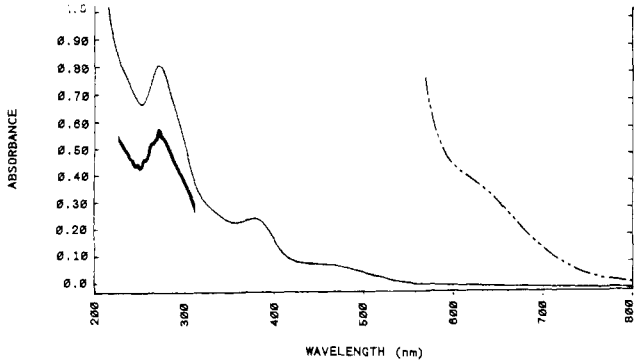

Figure 8. UV–vis spectrum of $W_2(CH_2Ph)_2(EtCCEt)_2(O\text{-}i\text{-}Pr)_4$ in pentane solvent. The solid and dashed lines represent 4.0 × 10^{-5} and 4.0 × 10^{-3} M concentrations, respectively. The inset between 230 and 300 nm shows the $\pi \rightarrow \pi^*$ fine structure of the CH_2Ph function in $W_2(CH_2Ph)_2(MeCCMe)_2(O\text{-}i\text{-}Pr)_4$.

modes were unequivocally identified. Agostic α-H interactions (low $\nu(C_\alpha\text{–}H_\alpha)$) were not detected for the α-H containing compounds **2**.

The electronic absorption data for selected representatives of **2** are listed in Table XIII, and a sample spectrum of 1,2-$W_2(CH_2Ph)_2(EtCCEt)_2(O\text{-}i\text{-}Pr)_4$ (**2**, R = CH_2Ph, R′ = R″ = Et) is shown in Figure 8. All four compounds display weak absorbances at ca. 640 nm with extinction coefficients of 130 M^{-1} cm^{-1} (average) most likely due to triplet transitions from tungsten-based orbitals.[9] The spectra for the two benzyl derivatives (R = CH_2Ph) contain strong absorbances at ca. 270 nm (ϵ 26 000 (average)), with the C_2Me_2 derivative showing considerable fine structure, assignable to $\pi \rightarrow \pi^*$ transitions of the arene rings.[52] An oxygen-to-metal charge-transfer band is observed for **2** (R = *n*-Pr, R′ = R″ = Me) at 240 nm (ϵ 20 000) comparable in energy and intensity with previously reported spectra for the $W_2(OR)_6$[16] and $W_3(\mu_3\text{-}O)(OR)_{10}$[53] compounds. The other transitions in the 350–500 nm range show alkyl group dependent shifts and could involve W–C(alkyl) orbitals.

$[W(\equiv CEt)(CH_2\text{-}t\text{-}Bu)(O\text{-}i\text{-}Pr)_2]_2$ and Pyridine Adducts. The low-temperature-limiting ^1H NMR spectrum of $[W(\equiv CEt)(CH_2\text{-}t\text{-}Bu)(O\text{-}i\text{-}Pr)_2]_2$ (**4**) at −92 °C in toluene-d_8 reveals the presence of two species in a ca. 4:1 ratio. These have been assigned to dimeric **4** and its monomer **4′**. The major set of resonances contains an ABX_3 methylene multiplet for the propylidyne Et group and two O-*i*-Pr methine resonances, which is consistent with the solid-state structure of **4** previously described. As the same is warmed, all resonances broaden and coalesce and, at 25 °C, sharpen to give a spectrum consistent with symmetrical monomer **4′** having nondiastereotopic propylidyne methylene hydrogens and one type of O-*i*-Pr ligand. A stacked plot of the variable-temperature ^1H NMR spectra of **4** is shown in Figure 9. These data are consistent with the equilibrium outlined in eq 7 and indicate that k_1 and k_{-1} are slow on the NMR time scale at −92 °C but rapid at room temperature.

$[W(\equiv CEt)(CH_2\text{-}t\text{-}Bu)(O\text{-}i\text{-}Pr)_2(py)]_2$ (**5**) is also fluxional in toluene-d_8, but the dynamic processes occurring in solution are more complicated than for **4**. When an NMR sample of **4** or **5** is spiked with excess pyridine (ca. 5 equiv), the room-temperature ^1H NMR spectrum (Figure 10) shows only one type of O-*i*-Pr ligand, which has diastereotopic methyl groups, and a quartet for the nondiast-

(52) Pavia, D. L.; Lampman, G. M.; Kriz, G. S. *Introduction to Spectroscopy*; W. B. Saunders: Philadelphia, PA, 1979; p 209.
(53) Chisholm, M. H.; Cotton, F. A.; Fang, A.; Kober, E. M. *Inorg. Chem.* **1984**, *23*, 749.

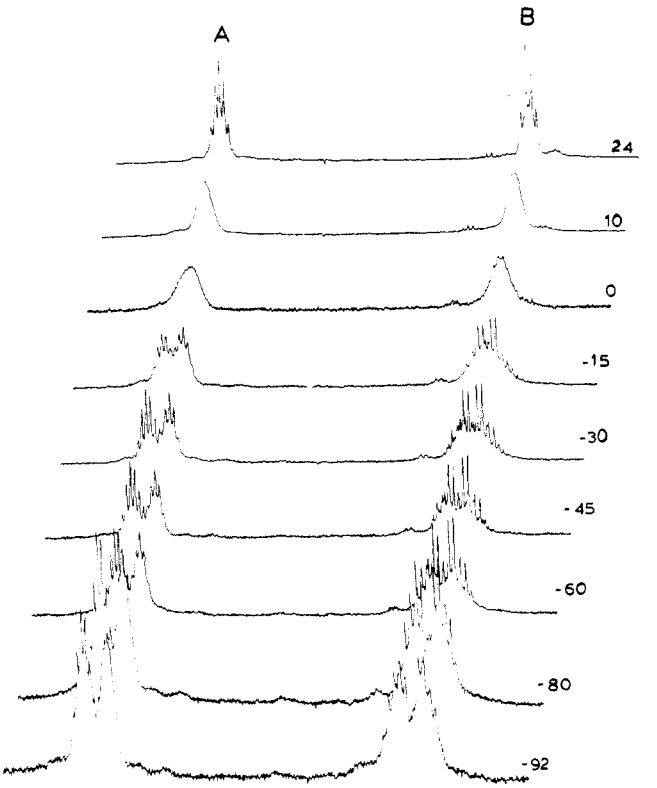

Figure 9. A stacked plot of the variable-temperature ^1H NMR spectra of $[W(\equiv CEt)(CH_2\text{-}t\text{-}Bu)(O\text{-}i\text{-}Pr)_2]_2$ recorded in toluene-d_8 solvent at 360 MHz. The displayed region shows the O-*i*-Pr methine resonances (A) and the propylidyne methylene resonances (B). The temperatures listed are in degrees centigrade, and each successive spectrum is offset ca. 0.02 ppm to the right.

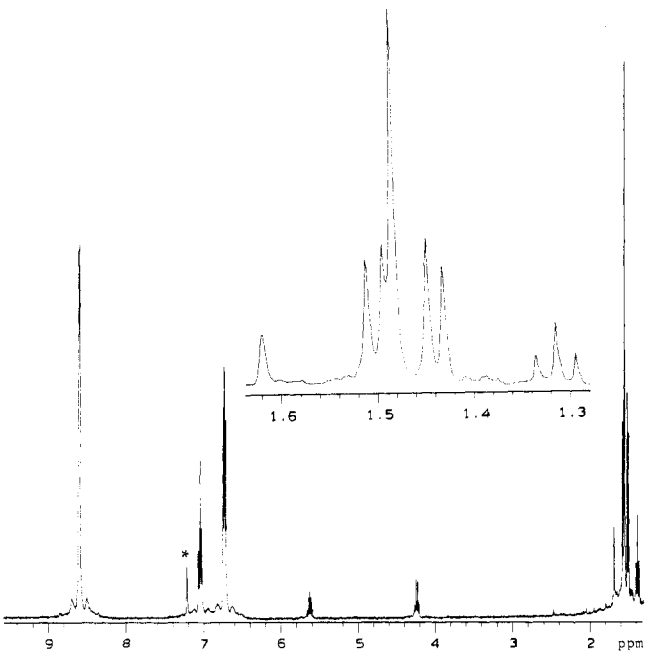

Figure 10. The ^1H NMR spectrum of $[W(\equiv CEt)(CH_2\text{-}t\text{-}Bu)(O\text{-}i\text{-}Pr)_2]_2$ in the presence of ca. 6 equiv of py. The spectrum was recorded at 22 °C and 360 MHz in benzene-d_6 solvent.

ereotopic propylidyne methylene hydrogens. These data indicate an octahedral bis(pyridine) monomer[54] (**9**), depicted by XIII, formed by the reaction shown in eq 10.

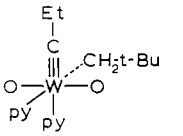

XIII, O = O-*i*-Pr

$$W(\equiv CEt)(CH_2\text{-}t\text{-}Bu)(O\text{-}i\text{-}Pr)_2 \underset{\mathbf{4'}}{} + \text{excess py} \rightarrow W(\equiv CEt)(CH_2\text{-}t\text{-}Bu)(O\text{-}i\text{-}Pr)_2(py)_2 \underset{\mathbf{9}}{} \quad (10)$$

1,1-W_2Me_2(μ-MeCCMe)(O-*t*-Bu)$_4$(py) and W_2Me(HCCH)(O-*t*-Bu)$_5$(py). The low-temperature-limiting ^1H NMR spectrum of 1,1-W_2Me_2(μ-MeCCMe)(O-*t*-Bu)$_4$(py) (**6**) in CD_2Cl_2 is consistent with the solid-state molecular structure previously described. No $^2J_{^{183}W\text{-}^1H}$ couplings were detected on the two Me resonances of the W-*Me* ligands due to the broadness of the lines at −80 °C in CD_2Cl_2. As the sample is warmed to −60 °C, the two Me resonances of the μ-MeCCMe ligand begin to broaden and, by −45 °C, coalesce into one broad signal. This dynamic behavior is consistent with a turnstile-type rotation of the two Me ligands and the terminal O-*t*-Bu ligand (O(28)) about W(2). A rotation of this type would generate a symmetry plane bisecting the Me substituents on the μ-MeCCMe ligand, thus making them equivalent. Unfortunately, **6** begins to decompose above −40 °C prohibiting further study of this process.

The room-temperature ^1H and $^{13}C\{^1H\}$ NMR spectrum of W_2Me(μ-HCCH)(O-*t*-Bu)$_5$(py) (**7**) are consistent with the previously described molecular structure depicted by XII. No fluxional processes were observed for **7** from −80 to 25 °C.

Conclusions

Compounds of formula 1,2-$W_2R_2(R'CCR'')_2$(O-*i*-Pr)$_4$ (**2**) can be prepared in high yield from reactions between 1,2-W_2R_2(O-*i*-Pr)$_4$($W\equiv W$) and small internal acetylenes (MeC≡CMe, MeC≡CEt, EtC≡CEt) where R = aryl or alkyl with or without β-hydrogen atoms. Compounds **2** have an unusual geometry with puckered W_2(O-*i*-Pr)$_2$ cores in the solid state arising from metal–ligand dominated π bonding. The alkyne ligands are tightly bound in terminal positions and are best considered as metallacyclopropene fragments. When the combined steric constraints of R, R′, and R″ become large, W≡W and C≡C metathesis reactions dominate over metallacyclopropene formation and compounds of formula $[W(\equiv CR')(R)(O\text{-}i\text{-}Pr)_2]_2$ are produced. 1,2-W_2Me_2(O-*t*-Bu)$_4$(py)$_2$ reacts with MeC≡CMe to form 1,1-W_2Me_2(μ-C_2Me_2)(O-*t*-Bu)$_4$(py) (**6**) in good yield. Compound **6** is derived from a metal-to-metal alkyl migration and represents the first fully characterized example of an alkyl migration at a $(W\equiv W)^{6+}$ center. 1,2-W_2Me_2(O-*t*-Bu)$_4$(py)$_2$ also reacts with ethyne producing W_2Me(μ-C_2H_2)(O-*t*-Bu)$_5$(py) (**7**) in a low yield. Compound **7** is apparently formed from an alkyl and alkoxide group disproportionation.

Compounds **2** undergo C–H activation and C–C coupling reactions under mild conditions of thermolysis or photolysis. Presumably an analogue of **2** is involved as an intermediate in the formation of HW_2(μ-C-*t*-Bu)(μ-C_4Me_4)(O-*i*-Pr)$_4$ in reaction 5, but changing the alkyne from MeC≡CMe to EtC≡CEt is sufficient to change the reaction to W≡W and C≡C metathesis as outlined by eq 6.

The lack of reactivity of related Mo_2R_2(O-*i*-Pr)$_4$ compounds with MeC≡CMe and EtC≡CEt is attributed to electronic factors that make the d^3–d^3 W_2^{6+} center a better

(54) (a) Chisholm, M. H.; Huffman, J. C.; Marchant, N. S. *J. Chem. Soc., Chem. Commun.* **1986**, 717. (b) Marchant, N. S. Ph.D. Thesis 1986, Indiana University, Bloomington, IN.

π-back-bonding metal center relative to Mo_2^{6+}.

Experimental Section

General Procedures. Standard Schlenk procedures and Vacuum Atmospheres Co. Dri-Lab Systems were used for all syntheses and sample manipulations. All solvents were distilled from Na/benzophenone and stored in solvent bottles over 4-Å molecular sieves.

The ^1H NMR spectra were recorded in dry and deoxygenated benzene-d_6, toluene-d_8, or methylene-d_2 chloride on either a Nicolet NT-360 (360 MHz) or a Varian XL300 (300 MHz) spectrometer. The data were calibrated against the residual protio impurities of the deuteriated solvents. The $^{13}C\{^1H\}$ NMR spectra were recorded in benzene-d_6 or toluene-d_8 on a Varian XL300 spectrometer at 75 MHz. The data were calibrated against the central resonance of C_6D_6 (128.0 ppm) or the central methyl resonance of $C_6D_5CD_3$ (20.4 ppm). Infrared spectra were obtained from either Nujol mulls between CsI plates or as KBr pellets by using a Perkin-Elmer 283 spectrophotometer and were referenced against the polystyrene absorbance at 1601 cm^{-1}. Electronic absorption spectra were recorded on a Hewlett-Packard 8450A spectrophotometer. Samples were run in pentane solutions vs a solvent blank by using matched 1-cm quartz cells.

Elemental analyses were performed by Alfred Bernhardt Mikroanalytisches Laboratorium, Elbach, West Germany and Schwarzkopf Microanalytical Laboratory, Woodside, NY.

Chemicals. The $M_2R_2(O\text{-}i\text{-}Pr)_4$ (where M = Mo, W) and $W_2R_2(O\text{-}t\text{-}Bu)_4$ compounds were prepared by published methods[24,25] except for $W_2(CH_2SiMe_3)_2(O\text{-}i\text{-}Pr)_4$ and $W_2(C_6H_4\text{-}p\text{-}Me)_2(O\text{-}t\text{-}Bu)_4$ which are described below. Isopropyl alcohol was distilled from Na and stored over 4-Å molecular sieves. *tert*-Butyl alcohol was distilled from CaH_2 as a 4.18 M benzene azeotrope and stored over 4-Å molecular sieves. The acetylenes were purchased commercially and used without further purification. CD_3OCD_3 was prepared by published methods.[55]

$W_2(CH_2SiMe_3)_2(O\text{-}i\text{-}Pr)_4$. A Schlenk reaction vessel was charged with 2.1 equiv of $LiCH_2SiMe_3$ (802 mg, 8.5 mmol) and toluene (20 mL) and stirred at 0 °C. $W_2Cl_2(NMe_2)_4$ (2.5 g, 4.1 mmol) was slowly added (ca. 20 min addition time) to the toluene/$LiCH_2SiMe_3$ slurry at 0 °C by using a solids addition tube. The reaction mixture gradually turned from yellow to brown over a 10-min period. The solution was warmed to room temperature and stirred for an additional 12 h. The solvent was then removed in vacuo and the oily residue extracted in hexane (2 × 10 mL) and filtered through a fine frit into a Schlenk flask. The brown hexane solution was then cooled to 0 °C and 4.1 equiv (1.28 mL, 16.6 mmol) *i*-PrOH added via syringe. The solution slowly turned red-orange after 30 min and was stirred for an additional 1 h at 0 °C. The solvent was then removed in vacuo and the red-orange microcrystalline residue extracted into pentane (15 mL) and filtered through a fine frit into a Schlenk flask. The volume of the solution was reduced to ca. 5 mL and cooled to −20 °C for 12 h. Orange-red crystals were harvested by removing the supernatant liquid via cannula and drying in vacuo (crystalline yield 2.17 g, 68%).

IR data (KBr pellet, cm^{-1}): 2988 (s), 2967 (s), 2948 (m), 1462 (w), 1448 (w), 1376 (m), 1366 (m), 1320 (m), 1255 (m), 1248 (s), 1161 (m), 1128 (m), 1111 (vs), 982 (vs), 947 (s), 892 (m), 854 (vs), 830 (m), 798 (s), 618 (s), 528 (vw).

$W_2(C_6H_4\text{-}p\text{-}Me)_2(O\text{-}t\text{-}Bu)_4$. In a Schlenk reaction vessel, $W_2(C_6H_4\text{-}p\text{-}Me)_2(NMe_2)_4$ (1.3 g, 1.8 mmol) was dissolved in hexane (15 mL) producing an orange-brown solution. *tert*-Butyl alcohol (4.1 equiv, 0.98 mL of 4.2 M *t*-BuOH/benzene azeotrope) was added via syringe at room temperature. The solution was stirred for 1 h at room temperature and turned dark red. The mixture was evaporated to dryness and the residue extracted into toluene (ca. 3 mL) and cooled to −20 °C. After 24 h, red-brown crystals (477 mg) were harvested by removing the supernatant liquid via cannula and drying the solid in vacuo. A second crystalline crop (100 mg) was isolated by recooling the supernatant liquid. Small amounts of $W_2(O\text{-}t\text{-}Bu)_6$ (ca. 5%) were detected in the crystalline sample, and elemental analysis was not attempted (crystalline yield 577 mg, 39%).

IR data (KBr pellet, cm^{-1}): 3022 (vw), 2965 (vs), 2915 (m), 2890 (m), 2858 (w), 1481 (w), 1468 (w), 1452 (w), 1386 (s), 1361 (s), 1236 (m), 1185 (m), 1165 (vs), 1024 (w), 972 (vs), 917 (m), 910 (m), 898 (s), 791 (s), 780 (m), 561 (vw).

$W_2(CH_2Ph)_2(MeCCMe)_2(O\text{-}i\text{-}Pr)_4$. In a Schlenk reaction vessel, $W_2(CH_2Ph)_2(O\text{-}i\text{-}Pr)_4$ (510 mg, 0.65 mmol) was dissolved in pentane (15 mL). The red-orange solution was frozen at −198 °C, and 2-butyne (2 equiv, 1.3 mmol) was condensed into the flask by using a calibrated vacuum manifold. The frozen mixture was rapidly warmed to 0 °C during which time the color turned lime green and then quickly to burnt orange after ca. 5 s. The solution was stirred at room temperature for 10 min, concentrated to ca. 3 mL total volume, and cooled to −20 °C for 48 h. Large, cubic crystals were collected by removing the supernatant liquid via cannula and drying in vacuo (crystalline yield 330 mg, 57%).

IR data (Nujol mull between CsI plates, cm^{-1}): 1928 (vw), 1918 (vw), 1593 (s), 1570 (w), 1488 (s), 1448 (m), 1362 (m), 1333 (s), 1261 (m), 1200 (m), 1164 (m), 1130 (s), 1121 (s), 1109 (vs), 1058 (vw), 1029 (w), 975 (s), 960 (s), 859 (m), 839 (m), 801 (m), 751 (m), 731 (m), 695 (s), 632 (w), 606 (m), 591 (w), 548 (m), 450 (m), 348 (vw), 311 (vw), 299 (w), 221 (vw).

Anal. Calcd for $W_2O_4C_{34}H_{54}$: C, 45.6; H, 6.0; N, 0.0. Found: C, 45.6; H, 6.0; N, <0.03.

$W_2(CH_2SiMe_3)_2(MeCCMe)_2(O\text{-}i\text{-}Pr)_4$. A procedure similar to that described for $W_2(CH_2Ph)_2(MeCCMe)_2(O\text{-}i\text{-}Pr)_4$ was followed. $W_2(CH_2SiMe_3)_2(O\text{-}i\text{-}Pr)_4$ (660 mg, 0.85 mmol) was used to produce the burnt orange crystalline product (crystalline yield 406 mg, 54%). No lime green color was observed during the rapid warming of the frozen mixture. The solution was only stirred for 10 min at room temperature following the addition of 2-butyne.

IR data (Nujol mull between CsI plates, cm^{-1}): 1330 (w), 1248 (m), 1238 (m), 1166 (m), 1131 (s), 1117 (vs), 997 (vs), 978 (w), 960 (m), 848 (s), 821 (m), 749 (w), 732 (w), 712 (m), 678 (w), 670 (w), 580 (w), 508 (w).

Anal. Calcd for $W_2O_4C_{28}Si_2H_{62}$: C, 38.0; H, 7.0. Found: C, 38.0; H, 6.8.

$W_2Me_2(MeCCMe)_2(O\text{-}i\text{-}Pr)_4$. In a Schlenk reaction vessel, $W_2Me_2(NMe_2)_4$ (50 mg, 0.09 mmol) was dissolved in hexane (10 mL) and frozen at −198 °C. 2-Butyne (2.2 equiv, 0.18 mmol) was condensed into the flask by using a calibrated vacuum manifold. The yellow solution was warmed to 0 °C during which time no color change occurred. The mixture was stirred at 0 °C, and *i*-PrOH (4.0 equiv, 28 μL) was added by using a microliter syringe. The solution quickly turned brown and then orange after 30 s. After the solution was stirred for 5 min at 0 °C, the solvent was removed in vacuo, the soluble residue extracted into C_6D_6 (1 mL), and the solution sealed in an NMR tube. Two compounds were observed by ^1H NMR, $W_2Me_2(MeCCMe)_2(O\text{-}i\text{-}Pr)_4$ (see Table XI) and $[(MeC{\equiv})W(O\text{-}i\text{-}Pr)_3(HNMe_2)]_2$,[29] in a ratio of ca. 9:1, respectively. Larger scale reactions led to the formation of greater relative quantities of $[(MeC{\equiv})W(O\text{-}i\text{-}Pr)_3(HNMe_2)]_2$, and attempts to separate the two compounds by fractional crystallization were unsuccessful. Attempts to prevent protolysis of the W–Me bonds by adding nonacidic Lewis bases such as PMe_3 or PEt_3 to the reaction mixture also proved unsuccessful.

$W_2(n\text{-}Pr)_2(MeCCMe)_2(O\text{-}i\text{-}Pr)_4$. In a Schlenk reaction vessel, $W_2(i\text{-}Pr)_2(NMe_2)_4$ (291 mg, 0.46 mmol) was dissolved in hexane (20 mL) and cooled to 0 °C, and *i*-PrOH (4.1 equiv, 146 μL) was added to the solution via microliter syringe. The mixture was stirred for 45 min at 0 °C during which time the color changed from light brown to dark brown. The solution was then degassed under vacuum (to remove all $HNMe_2$) and frozen to −198 °C, and 2-butyne (2.1 equiv, 0.197 mmol) was added to the flask by using a calibrated vacuum manifold. The mixture was rapidly warmed to 0 °C and stirred for 10 min. The color quickly changed from brown to dirty green to orange as the solution was warmed. The volume of the reaction mixture was reduced to ca. 3 mL and cooled to −20 °C for 48 h. Brown crystals were harvested by removing the supernatant liquid via cannula and drying in vacuo (crystalline yield 126 mg, 34%). No W–(*i*-Pr) products were detected by ^1H NMR. Reactions employing $W_2(n\text{-}Pr)_2(NMe_2)_4$ also yielded $W_2(n\text{-}Pr)_2(MeCCMe)_2(O\text{-}i\text{-}Pr)_4$ under the same reaction conditions.

IR data (KBr pellet, cm^{-1}): 2984 (vs), 2973 (vs), 2961 (vs), 2946 (s), 2930 (s), 1461 (m), 1450 (s), 1384 (m), 1376 (s), 1362 (vs), 1330

(55) Sandstrom, J. *Dynamic NMR Spectroscopy*; Academic: New York, 1982; p 66.

Table XI. ^1H and $^{13}C\{^1H\}$ NMR Data[a]

compound	^1H NMR[b]	$^{13}C\{^1H\}$ NMR[c]
$W_2(CH_2SiMe_3)_2(O\text{-}i\text{-}Pr)_4$ (benzene-d_6, 22 °C)	OC*H*Me$_2$ (5.88, sept, 1 H, 6.1); C*H*$_2$SiMe$_3$ (1.95, s, 1 H, $^2J_{^{183}W\text{-}^1H}$ = 11.0); OCH*Me*$_2$ (1.50, d, 6 H, 6.1), (1.47, d, 6 H, 6.1); CH$_2$Si*Me*$_3$ (0.15, s, 9 H)	OCHMe$_2$ (89.49); CH$_2$SiMe$_3$ (42.6); OCH*Me*$_2$ (27.4), (26.6); CH$_2$Si*Me*$_3$ (2.2)
$W_2(C_6H_4\text{-}p\text{-}Me)_2(O\text{-}t\text{-}Bu)_4$ (benzene-d_6, 22 °C)	C$_6$H$_4$-*p*-Me, ortho (7.90, d, 2 H, 7.9); meta (7.24, d, 2 H, 7.6); C$_6$H$_4$-*p*-*Me* (2.25, s, 3); O-*t*-*Bu* (1.50, s, 18)	*C*$_6$H$_4$-*p*-Me, ipso (189.8), ortho (137.7), meta (135.5); O*C*Me$_3$ (80.9); OC*Me*$_3$ (33.6); C$_6$H$_4$-*p*-*Me* (21.4)
$W_2(CH_2Ph)_2(MeCCMe)_2(O\text{-}i\text{-}Pr)_4$ (toluene-d_8, 22 °C)	CH$_2$*Ph*, ortho (7.52, d, 2 H, 7.2), meta (7.18, dd, 2 H, 7.2), para (6.87, t, 1 H, 7.2); OC*H*Me$_2$ (4.72, sept, 1 H, 6.1); C*H*$_2$Ph (3.92, d, 1 H, 10.3, $^2J_{^{183}W\text{-}^1H} \approx 9$), (3.77, d, 1 H, 10.3, $^2J_{^{183}W\text{-}H} \approx 10$); C$_2$*Me*$_2$ (3.11, s, 6 H); OC*H*Me$_2$ (2.85, sept, 1 H, 6.1); OCH*Me*$_2$ (1.24, d, 3 H, 6.1), (1.20, d, 3 H, 6.1), (0.51, d, 3 H, 6.1), (0.42, d, 3 H, 6.1)	*C*$_2$Me$_2$ (201.9, $^1J_{^{183}W\text{-}^{13}C}$ = 46); CH$_2$*Ph*, ipso (152.2), ortho (129.0), meta (ca. 128), para (122.5); OCHMe$_2$ (78.0, $^2J_{^{183}W\text{-}^{13}C}$ = 10), (75.4); *C*H$_2$Ph (40.3, $J_{^{183}W\text{-}^{13}C}$ = 68); OCH*Me*$_2$ (26.2), (25.8), (24.3), (23.5); C$_2$*Me*$_2$ (21.0)
$W_2(CH_2SiMe_3)_2(MeCCMe)_2(O\text{-}i\text{-}Pr)_4$ (benzene-d_6, 22 °C)	OC*H*Me$_2$ (4.54, sept, 1 H, 6.1), (3.92, sept, 1 H, 6.1); C$_2$*Me*$_2$ (3.24, s, 6 H); C*H*$_2$SiMe$_3$ (1.97, d, 1 H, 12.3, $^2J_{^{183}W\text{-}^1H} \approx 9$), (1.63, d, 1 H, 12.3, $^2J_{^{183}W\text{-}^1H} \approx 9$); OCH*Me*$_2$ (1.12, d, 3 H, 6.1), (1.05, d, 3 H, 6.1), (0.88, d, 3 H, 6.1), (0.67, d, 3 H, 6.1); CH$_2$Si*Me*$_3$ (0.29, s, 9 H)	*C*$_2$Me$_2$ (200.4, $^1J_{^{183}W\text{-}^{13}C}$ = 43); OCHMe$_2$ (77.6, $^2J_{^{183}W\text{-}^{13}C}$ = 12), (75.1); *C*H$_2$SiMe$_3$ and OCH*Me*$_2$ (26.5), (25.1), (24.6), (23.7), 23.3); C$_2$*Me*$_2$ (20.7); CH$_2$Si*Me*$_3$ (3.3)
$W_2(Me)_2(MeCCMe)_2(O\text{-}i\text{-}Pr)_4$ (benzene-d_6, 22 °C)	OC*H*Me$_2$ (4.44, sept, 1 H, 6.1), (3.72, sept, 1 H, 6.1); C$_2$*Me*$_2$ (3.18, s, 6 H); W-*Me* (1.75, s, 3 H); OCH*Me*$_2$ (1.30, d, 3 H, 6.1), (0.95, d, 3 H, 6.1), (0.81, d, 3 H, 6.1), (0.76, d, 3 H, 6.1)	N/R
$W_2(n\text{-}Pr)_2(MeCCMe)_2(O\text{-}i\text{-}Pr)_4$ (benzene-d_6, 22 °C)	OC*H*Me$_2$ (4.58, sept, 1 H, 6.5), (3.67, sept, 1 H, 6.5); C$_2$*Me*$_2$ (3.16, s, 6 H); C*H*$_2$CH$_2$CH$_3$ (2.54, m, 1 H), (2.31, m, 1 H); CH$_2$C*H*$_2$CH$_3$ (2.09, m, 1 H), (1.90, m, 1 H); CH$_2$CH$_2$C*H*$_3$ (1.46, t, 3 H, 7.2); OCH*Me*$_2$ (1.30, d, 3 H, 6.5), (0.91, d, 3 H, 6.5), (0.84, d, 3 H, 6.5), (0.70, d, 3 H, 6.5)	*C*$_2$Me$_2$ (201.6, $^1J_{^{183}W\text{-}^{13}C}$ = 43); O*C*HMe$_2$ (77.4, $^2J_{^{183}W\text{-}^{13}C}$ = 10), (72.4); *n*-Pr, α (43.1, $^1J_{^{183}W\text{-}^{13}C}$ = 78); β (21.8, $^2J_{^{183}W\text{-}^{13}C} \approx 8$); OCH*Me*$_2$, *n*-Pr [$\gamma$] and C$_2$*Me*$_2$ (26.7), (25.9), (25.3), (24.6), (24.0), (20.1)
$W_2(i\text{-}Bu)_2(MeCCMe)_2(O\text{-}i\text{-}Pr)_4$ (benzene-d_6, 22 °C)	OC*H*Me$_2$ (4.52, sept, 1 H, 6.1), (3.68, sept, 1 H, 6.3); C$_2$*Me*$_2$ (3.18, s, 6 H); *i*-Bu, α (2.62, m, 1 H), (2.35, m 1 H); β (2.28, m, 1 H); γ (1.42, d, 3 H, 6.6), (1.29, d, 3 H, 6.6); OCH*Me*$_2$ (1.21, d, 3 H, 6.1), (1.03, d, 3 H, 6.1), (0.84, d, 3 H, 6.1), (0.69, d, 3 H, 6.1)	*C*$_2$Me$_2$ (201.5, $^1J_{^{183}W\text{-}^{13}C}$ = 44); O*C*HMe$_2$ (77.4, $^2J_{^{183}W\text{-}^{13}C}$ = 12), (73.9); *C*H$_2$CHMe$_2$ (48.6, $^1J_{^{183}W\text{-}^{13}C}$ = 75); C$_2$*Me*$_2$ (24.7); *i*-Bu [β and γ], OCH*Me*$_2$ (32.4, relative intensity 2), (28.7), (28.0), (26.3), (24.0), (20.4)
$W_2(Et)_2(MeCCMe)_2(O\text{-}i\text{-}Pr)_4$ (benzene-d_6, 22 °C)	OC*H*Me$_2$ (4.54, sept, 1 H, 6.3), (3.68, sept, 1 H, 6.2); C$_2$*Me*$_2$ (3.16, s, 6 H); C*H*$_2$Me (2.58, m, 1 H), (2.32, m, 1 H); CH$_2$*Me* (1.93, t, 3 H, 7.8); OCH*Me*$_2$ (1.29, d, 3 H, 6.2), (0.92, d, 3 H, 6.2), (0.84, d, 3 H, 6.1), (0.70, d, 3 H, 6.2)	*C*$_2$Me$_2$ (201.9, $^1J_{^{183}W\text{-}^{13}C}$ = 44); O*C*HMe$_2$ (77.4), (72.4); *C*H$_2$Me (31.9, $^1J_{^{183}W\text{-}^{13}C}$ = 78); CH$_2$*Me*, OCH*Me*$_2$, and C$_2$*Me*$_2$ (25.7), (25.1), (24.3), (24.0), (19.8), (17.5)
$W_2(C_6H_5)_2(MeCCMe)_2(O\text{-}i\text{-}Pr)_4$ ^1H NMR (benzene-d_6, 22 °C); $^{13}C\{^1H\}$ NMR (toluene-d_8, 22 °C)	C$_6$*H*$_5$, ortho (8.18, d, 2 H, 7.2), meta (7.55, dd, 2 H, 7.2), para (7.32, t, 1 H, 7.2); OC*H*Me$_2$ (4.10, sept, 1 H, 6.5), (3.90, sept, 1 H, 6.5); C$_2$*Me*$_2$ (3.15, s, 6 H); OCH*Me*$_2$ (0.95, d, 3 H, 6.5), (0.80, d, 3 H, 6.5), (0.79, d, 3 H, 6.5), (0.63, d, 3 H, 6.5)	*C*$_2$Me$_2$ (200.8, $^1J_{^{183}W\text{-}^{13}C} \approx 40$); *C*$_6H_5$, ipso (173.6, $^1J_{^{183}W\text{-}^{13}C}$ = 100); ortho (139.8); meta (126.6); para (125.7); OCHMe$_2$ (75.6), (78.6); OCH*Me*$_2$ and C$_2$*Me*$_2$ (27.3), (24.4), (23.2)
$W_2(C_6H_4\text{-}p\text{-}Me)_2(MeCCMe)_2(O\text{-}i\text{-}Pr)_4$ ^1H NMR (benzene-d_6, 22 °C); $^{13}C\{^1H\}$ NMR (toluene-d_8, 22 °C)	C$_6$*H*$_4$-*p*-Me, ortho (8.12, d, 2 H, 7.9), meta (7.37, d, 2 H, 7.9); OC*H*Me$_2$ (4.14, sept, 1 H, 6.1), (3.93, sept, 1 H, 6.1); C$_2$*Me*$_2$ (3.18, s, 6 H); C$_6$H$_4$-*p*-*Me* (2.36, s, 3 H); OCH*Me*$_2$ (0.99, d, 3 H, 6.1), (0.82, d, 3 H, 6.1), (0.82, d, 3 H, 6.1)	*C*$_2$Me$_2$ (201.5); *C*$_6$H$_4$-*p*-Me, ipso (170.3, $^1J_{^{183}W\text{-}^{13}C}$ = 103), ortho (140.2), meta (134.5), para (127.7); OCHMe$_2$ (78.6, $^2J_{^{183}W\text{-}^{13}C}$ = 10), (75.6); OCH*Me*$_2$ (27.4), (24.5), (24.4), (23.2); C$_2$*Me*$_2$ (21.5); C$_6$H$_4$-*p*-*Me* (~20.7, shoulder on toluene-d_8 Me resonance)
$W_2(CH_2Ph)_2(MeCCEt)_2(O\text{-}i\text{-}Pr)_4$ (benzene-d_6, 22 °C)	CH$_2$*Ph*, ortho (7.60, d, 2 H, 7.0), meta (7.24, dd, 2 H, 7.3), para (6.93, t, 1 H, 7.10); OC*H*Me$_2$ (4.71, sept, 1 H, 6.5), (2.84, sept, 1 H, 6.1); C*H*$_2$Ph (3.99, d, 1 H, 10.4), (3.86, d, 1 H, 10.4); MeCCC*H*$_2$Me (3.56, q, 2 H, ~7); *Me*CCCH$_2$Me (3.27, s, 3 H); MeCCCH$_2$*Me* (1.41, t, 3 H, 7.4); OCH*Me*$_2$ (1.26, d, 3 H, 6.4), (1.24, d, 3 H, 6.4), (0.52, d, 3 H, 6.1), (0.44, d, 3 H, 6.4)	Me*C*CEt (204.2), (200.6); CH$_2$*Ph*, ipso (161.4), ortho (152.1), meta (129.1), para (122.5); O*C*HMe$_2$ (78.0, $^2J_{^{183}W\text{-}^{13}C}$ = 10), (75.4); *C*H$_2$Ph (39.6, $^1J_{^{183}W\text{-}^{13}C}$ = 68); OCH*Me*$_2$ (26.3), (25.9), (24.3), (23.4); *Me*C*C*Et (31.6), (22.2), (14.3)
$W_2(n\text{-}Pr)_2(MeCCEt)_2(O\text{-}i\text{-}Pr)_4$ (benzene-d_6, 22 °C)	OC*H*Me$_2$ (4.56, d, 1 H, 6.0), (3.69, d, 1 H, 6.0); MeCCC*H*$_2$CH$_3$ (3.56, m, 2 H); *Me*CCEt (3.29, s, 3 H); *n*-Pr, α (2.56, m, 1 H), (2.29, td, 1 H); *n*-Pr, β (2.30, m, 1 H), (1.88, m, 1 H); MeCCCH$_2$*CH*$_3$ (1.48, t, 3 H, 7.4); *n*-Pr, γ (1.46, t, 3 H, 6.9); OCH*Me*$_2$ (1.31, d, 3 H, 6.2), (0.94, d, 3 H, 6.0), (0.85, d, 3 H, 6.0), (0.73, d, 3 H, 6.2)	Me*C*CEt (204.6, $^1J_{^{183}W\text{-}^{13}C}$ = 42), (200.7); OCHMe$_2$ (77.3, $^2J_{^{183}W\text{-}^{13}C}$ = 10), (72.5); *n*-Pr, α (42.6, $^1J_{^{183}W\text{-}^{13}C}$ = 78); *n*-Pr [β and γ], *Me*CC*H*$_2$*Me*, and OCH*Me*$_2$ (30.6), (26.5), (25.8), (25.1), (24.2), (23.9), (21.6), (20.6), (14.5)

Table XI (Continued)

compound	^{1}H NMR[b]	^{13}C{^{1}H} NMR[c]
$W_2(i\text{-Bu})_2(EtCCEt)_2(O\text{-}i\text{-Pr})_4$ (benzene-d_6, 22 °C)	OC*H*Me$_2$ (4.50, sept, 1 H, 6.4), (ca. 3.75, sept—overlap with C_2Et_2 multiplet); $C_2(CH_2Me)_2$ (3.70, m, 4 H); *i*-Bu, α (2.60, dd, 1 H), (2.32, dd, 1 H); β (2.19, m, 1 H); $C_2(CH_2Me)_2$ (1.44, t, 6 H, 7.5); *i*-Bu [γ] and OCH*Me*$_2$ (1.43, d, 3 H, ~6), (1.27, d, 3 H, 6.4), (1.21, d, 3 H, 6.3), (1.09, d, 3 H, 6.4), (0.89, d, 3 H, 6.1), (0.76, d, 3 H, 6.1)	C_2Et_2 (203.8, $^1J_{^{183}W-^{13}C}$ = 40); OCHMe$_2$ (77.4, $^2J_{^{183}W-^{13}C}$ = 11), (74.3); *i*-Bu, α (47.6, $^1J_{^{183}W-^{13}C}$ = 83); *i*-Bu [β, γ], OCH*Me*$_2$, and C_2Et_2 (32.2), (30.2), (29.0), (27.7), (26.5), (25.1), (24.7), (23.9), (15.0)
$W_2(CH_2Ph)_2(EtCCEt)_2(O\text{-}i\text{-Pr})_4$ (benzene-d_6, 22 °C)	CH_2*Ph*, ortho (7.60, d, 2 H, 7.2); meta (7.24, dd, 2 H, 7.2); para (6.93, t, 1 H, 7.2); OC*H*Me$_2$ (4.72, sept, 1 H, 6.1); C*H*$_2$Ph (3.96, d, 1 H, 10.1), (3.87, d, 1 H, 10.1, $^2J_{^{183}W-^1H}$ = 7.0); $C_2(CH_2Me)_2$ (3.73, m, 2 H), (3.62, m, 2 H); OC*H*Me$_2$ (2.85, sept, 1 H, 6.1); $C_2(CH_2Me)_2$ (1.37, t, 6 H, 7.2); OCH*Me*$_2$ (1.29, d, 3 H, 6.1), (1.24, d, 3 H, 6.1), (0.53, d, 3 H, 6.1), (0.47, d, 3 H, 6.1)	$C_2(CH_2Me)_2$ (203.4, $J_{^{183}W-^{13}C}$ = 43); CH_2*Ph*, ipso (152.0), ortho (129.1), meta (127.8), para (122.5); OCHMe$_2$ (78.1, $J_{^{183}W-^{13}C}$ = 10), (75.6); *C*H$_2$Ph (39.3, $J_{^{183}W-^{13}C}$ = 68); $C_2(CH_2Me)_2$ (31.0); OCH*Me*$_2$ (26.6), (26.2), (24.5), (23.4); $C_2(CH_2Me)_2$ (14.9)
$W_2(CH_2SiMe_3)_2(EtCCEt)_2(O\text{-}i\text{-Pr})_4$ (toluene-d_8, 22 °C)	OC*H*Me$_2$ (4.51, sept, 1 H, 6.1), (3.99, sept, 1 H, 6.1); $C_2(CH_2Me)_2$ (3.72, m, 2 H), (3.63, m, 2 H); C*H*$_2$SiMe$_3$ (1.87, d, 1 H, 12.6), (1.57, d, 1 H, 12.6, $^2J_{^{183}W-^1H}$ = 8.4); $C_2(CH_2Me)_2$ (1.45, t, 6 H, 7.6); OCH*Me*$_2$ (1.17, d, 3 H, 6.1), (1.07, d, 3 H, 6.1), (0.92, d, 3 H, 6.1), (0.77, d, 3 H, 6.1); CH_2SiMe_3 (0.30, s, 9 H, $^2J_{^{29}Si-^1H}$ = 5.6)	$C_2(CH_2Me)_2$ (202.4, $^1J_{^{183}W-^{13}C}$ = 41); OCHMe$_2$ (77.6, $^2J_{^{183}W-^{13}C}$ = 12), (75.4); $C_2(CH_2Me)_2$ (30.7); OCH*Me*$_2$ (26.9), (25.4), (24.9), (23.9); *C*H$_2$SiMe$_3$ (23.0, $^1J_{^{183}W-^{13}C}$ = 74, $^1J_{^{29}Si-^{13}C}$ = 44); $C_2(CH_2Me)_2$ (15.3); CH_2SiMe_3 (3.8, $^1J_{^{29}Si-^{13}C}$ = 48)
$W_2(Me)_2(EtCCEt)_2(O\text{-}i\text{-Pr})_4$ (benzene-d_6, 22 °C)	OC*H*Me$_2$ (4.46, sept, 1 H, 6.1), (~3.7, overlap with C_2Et_2 resonances); $C_2(CH_2Me)_2$ (~3.7, m); W-*Me* (1.75, s, 3 H, $^2J_{^{183}W-^1H}$ = 5.0); $C_2(CH_2Me)$ (1.42, t, 6 H, 9.0); OCH*Me*$_2$ (1.33, d, 3 H, 6.1), (1.00, d, 3 H, 6.1), (0.86, d, 3 H, 6.1), (0.82, d, 3 H, 6.1)	N/R
$W_2(C_6H_4\text{-}p\text{-Me})_2(MeCCMe)_2(O\text{-}t\text{-Bu})_4$ (benzene-d_6, 22 °C)	C_6H_4-*p*-Me, ortho (8.38, d, 2 H, 7.3); meta (7.32, d, 2 H, 7.3); C_2Me_2 (3.40, s br, 3 H), (3.10, s br, 3 H); C_6H_4-*p*-*Me* (2.33, s, 3 H); OC*Me*$_3$ (1.02, s, 9 H), (0.94, s, 9 H)	C_6H_4-*p*-Me, ipso (171.0, $^2J_{^{183}W-^{13}C}$ = 101); ortho (143.7), meta (135.0), para (126.5); O*C*Me$_3$ (85.7), (82.7); OC*Me*$_3$ (32.6), (30.4); C_6H_4-*p*-*Me* (21.7)
$[W(\equiv CEt)(CH_2\text{-}t\text{-Bu})(O\text{-}i\text{-Pr})_2]_2$ ^{1}H NMR (benzene-d_6, 25 °C); ^{13}C{^{1}H} NMR (toluene-d_8, 22 °C)	OC*H*Me$_2$ (5.32, sept, 2 H, 6.1); OC*H*$_2$Me (4.06, q, 2 H, 7.6); OCH*Me*$_2$ (1.4, d-br); CH_2-*t*-*Bu* (1.38, s, 9 H); CCH_2Me (1.18, t, 3 H, 7.6)	W≡*C*Et (278.3, $^1J_{^{183}W-^{13}C}$ = 292); OCHMe$_2$ (80.8), (77.4), (75.4); *C*H$_2$-*t*-Bu (40.6, $^1J_{^{183}W-^{13}C}$ = 51.4); CH_2CMe_3 (34.5); CH_2CMe_3, OCH*Me*$_2$, and CCH_2Me (35.4), (34.3), (31.6), (27.2), (17.8)
$[W(\equiv CEt)(CH_2\text{-}t\text{-Bu})(O\text{-}i\text{-Pr})_2(py)]_2$ ^{1}H NMR (benzene-d_6, 22 °C); ^{13}C{^{1}H} NMR (toluene-d_8, 22 °C)	py, ortho (8.78, s-br, 2 H), para (6.91, t, 1 H, 7.6), meta (6.64, dd, 2 H, ~7); OC*H*Me$_2$ (5.48, br, 2 H); CCH_2Me (4.2, br), (4.3, br) combined intensities ≈ 2 H; OCH*Me*$_2$ (1.51, d br, ~12 H, ~6); CH_2CMe_3 (1.44, s, 9 H)	W≡*C*Et (277.3); py (150.2), (136.6), (123.4); OCHMe$_2$ (84.1), (74.7), (74.6); CH_2-*t*-Bu (39.1, $^1J_{^{183}W-^{13}C}$ = 51); CH_2CMe_3, OCH*Me*$_2$, and C*Et* (35.5), (35.2), (27.7), (27.5), (19.0), (18.9)
1,1-$W_2(Me)_2(\mu\text{-MeCCMe})(O\text{-}t\text{-Bu})_4(py)$ (methylene-d_2 chloride, −80 °C]	py, ortho (8.58, d, 1 H, 6.0), (8.51, d, 1 H, 6.0), para (7.79, t, 1 H, 6.0), meta (7.38, m, 2 H); C_2Me_2 (3.64, s, 3 H), (3.42, s, 3 H); O-*t*-*Bu* (1.68, s, 9 H), (1.16, s, 9 H), (0.76, s, 9 H), (0.63, s, 9 H); W-*Me* (1.17, s, 3 H), (0.65, s, 3 H)	N/R
$W_2(Me)(\mu\text{-HCCH})(O\text{-}t\text{-Bu})_6(py)$ (toluene-d_8, −65 °C)	py, ortho (9.39, d, 1 H, 6.0), (8.31, d, 1 H, 6.0), para (6.58, t, 1 H, 6.0), meta (6.30, t, 1 H, 6.0), (6.18, t, 1 H, 6.0); C_2H_2 (5.91, s, 2 H); OC*Me*$_3$ (2.04, s, 9 H), (1.64, s, 18 H), (1.08, s, 18 H); W-*Me* (1.93, s, 3 H)	C_2H_2 (152.4); O*C*Me$_3$ (87.6), (80.2), (79.3) with relative intensities of 1:2:2, respectively; W-*Me* (31.0)

[a] ^{1}H NMR data are reportd as follows: assignment (chemical shift in ppm, multiplicity, relative intensity, H–H coupling constant in Hz, heteronuclear coupling constants in Hz). ^{13}C{^{1}H} NMR data are reported as follows: assignment (chemical shift in ppm, heteronuclear coupling constants in Hz). [b] Abbreviations: s, singlet; d, doublet; t, triplet; sept, septet; br, broad; dd, doublet of doublets; td, triplet of doublets. [c] Assignments were based on proton-coupled ^{13}C NMR experiments when ambiguities existed.

(s), 1166 (s), 1146 (s), 1131 (s), 1115 (vs), 1040 (w), 983 (vs), 956 (vs), 854 (s), 836 (s), 789 (vw), 684 (vw), 629 (vw), 608 (s), 559 (m), 451 (m).

Anal. Calcd for $W_2O_4C_{26}H_{54}$: C, 39.1; H, 6.8. Found: C, 38.6; H, 6.5.

$W_2(i\text{-Bu})_2(MeCCMe)_2(O\text{-}i\text{-Pr})_4$. In a Schlenk reaction vessel, $W_2(i\text{-Bu})_2(NMe_2)_4$ (850 mg, 1.29 mmol) was dissolved in hexane (12 mL) forming a yellow-brown solution. *i*-PrOH (4.1 equiv, 407 μL) was added to the solution by using a microliter syringe. The mixture was stirred at room temperature for 1 h during which time it turned orange-brown. The solution was then degassed, to remove the liberated $HNMe_2$, and frozen at −198 °C. 2-Butyne (2.1 equiv) was added to the flask at −198 °C by using a calibrated vacuum manifold. The frozen mixture was rapidly warmed to room temperature and stirred for 5 min. As the solution warmed, it turned from orange-brown to dirty brown and finally to burnt orange after 30 s. The reaction mixture was then evaporated to dryness, extracted into pentane (ca. 5 mL), and filtered through a fine frit. The solution was then concentrated to ca. 2 mL and cooled to −20 °C. After 24 h, large orange-brown crystals were isolated by removing the supernatant liquid via cannula and drying in vacuo (crystalline yield 463 mg, 44%).

IR data (KBr pellet, cm^{-1}): 1621 (vw), 1458 (m), 1449 (m), 1381 (m), 1373 (s), 1359 (s), 1328 (m), 1151 (s), 1117 (vs), 1111 (vs), 994 (s), 989 (s), 970 (s), 952 (s), 851 (m), 832 (m), 394 (w).

$W_2Et_2(MeCCMe)_2(O\text{-}i\text{-Pr})_4$. In a Schlenk reaction vessel, $W_2Et_2(NMe_2)_4$ (300 mg, 0.49 mmol) was dissolved in hexane (12 mL) and cooled to −20 °C. *i*-PrOH (4.05 equiv, 156 μL, 2.02 mmol) was slowly added to the yellow-brown solution at −20 °C. The mixture was stirred for a total of 30 min at −20 °C and was degassed every ca. 10 min to remove $HNMe_2$ produced during alcoholysis. The color slowly turned to red-brown over the 30-min

reaction period. The resulting solution was frozen at −198 °C and 2-butyne (2.1 equiv, 1.0 mmol) condensed into the flask by using a calibrated vacuum manifold. The frozen mixture was rapidly warmed to 0 °C and stirred at room temperature for 5 min. The resulting orange solution was evaporated to dryness, extracted into pentane (8 mL), and filtered through a fine frit. The solution was concentrated to ca. 2 mL and cooled to −78 °C. After 48 h, 88 mg of microcrystalline solid was isolated by removing the supernatant liquid via cannula and drying in vacuo (crystalline yield 88 mg, 23%).

IR data (KBr pellet, cm^{-1}): 2965 (s), 2924 (m), 2892 (m), 2850 (m), 1610 (w, br), 1443 (m), 1383 (vs), 1372 (s), 1361 (s), 1326 (w), 1260 (w), 1161 (m), 1112 (vs), 980 (s), 951 (s), 850 (m), 840 (m), 808 (m), 600 (w).

$W_2(C_6H_5)_2$(MeCCMe)$_2$(O-*i*-Pr)$_4$. In a Schlenk reaction vessel, $W_2(C_6H_5)_2(O\text{-}i\text{-}Pr)_4(HNMe_2)$ (303 mg, 0.37 mmol) was dissolved in pentane (20 mL) and frozen at −198 °C. 2-Butyne (2.0 equiv, 0.74 mmol) was condensed into the flask by using a calibrated vacuum manifold. The frozen mixture was then rapidly warmed to 0 °C during which time the color immediately changed from brown to fluorescent green and faded to burnt orange after 10 s. The solution was stirred for 5 min at 0 °C and the volume reduced to ca. 2 mL and cooled to −20 °C for 48 h. Orange-brown crystals were harvested by removing the supernatant liquid via cannula and drying in vacuo (crystalline yield 179 mg, 55%).

$W_2(C_6H_4$-*p*-Me$)_2$(MeCCMe$)_2$(O-*i*-Pr$)_4$. A procedure identical with that described for $W_2(C_6H_5)_2(MeCCMe)_2(O\text{-}i\text{-}Pr)_4$ was followed except $W_2(C_6H_4\text{-}p\text{-}Me)_2(O\text{-}i\text{-}Pr)_4(HNMe_2)$ was employed as starting material (crystalline yield ca. 40%).

IR data (KBr pellet, cm^{-1}): 3028 (w), 2987 (s), 2958 (s), 2950 (s), 2930 (m), 1481 (w), 1461 (w), 1459 (w), 1388 (m), 1380 (m), 1367 (m), 1328 (m), 1260 (vw), 1180 (w), 1162 (m), 1112 (vs), 1015 (m), 988 (vs), 960 (m), 937 (s), 856 (m), 843 (m), 830 (m), 802 (m), 602 (m), 561 (w), 500 (w), 449 (w), 381 (w).

Anal. Calcd for $W_2O_4C_{34}H_{54}$: C, 45.6; H, 6.0. Found: C, 45.0; H, 6.3.

$W_2(CH_2Ph)_2$(MeCCEt$)_2$(O-*i*-Pr$)_4$. In a Schlenk reaction vessel, $W_2(CH_2Ph)_2(O\text{-}i\text{-}Pr)_4$ (250 mg, 0.32 mmol) was dissolved in pentane (12 mL) and cooled to 0 °C. 2-Pentyne (2.05 equiv, 62 μL, 0.67 mmol) was added to the red-brown solution via microliter syringe. The solution immediately turned dark brown upon addition of 2-pentyne and then lightened to a burnt orange color after ca. 40 s. The mixture was stirred at room temperature for 30 min. The volume was then reduced to 2 mL and the solution cooled to −20 °C. After 7 days, an orange microcrystalline powder was isolated by removing the supernatant liquid via cannula and drying in vacuo (yield 89 mg, 30%).

W_2(*n*-Pr$)_2$(MeCCEt$)_2$(O-*i*-Pr). A Schlenk flask was charged with $W_2(i\text{-}Pr)_2(NMe_2)_4$ (350 mg, 0.57 mmol) and pentane (10 mL) and cooled to 0 °C. *i*-PrOH (4.1 equiv, 181 μL, 2.34 mmol) was added to the orange-brown solution via microliter syringe, and the mixture was stirred at 0 °C. The solution slowly darkened as the reaction proceeded and was degassed every 15 min to remove the liberated $HNMe_2$. After 45 min, 2-pentyne (2.1 equiv, 116 μL, 1.20 mmol) was added via syringe to the reaction mixture at 0 °C. The solution turned brown-orange after ca. 30 s and was stirred an additional 45 min at 0 °C. The volume of the solution was then reduced to ca. 2 mL and cooled to −20 °C. After 12 h, orange-brown crystals were harvested by removing the supernatant liquid via cannula and drying in vacuo (crystalline yield 134 mg, 29%).

Anal. Calcd for $W_2O_4C_{28}H_{58}$: C, 40.7; H, 7.0. Found: C, 42.4; H, 6.8. The compound may have thermally decomposed before the analysis was undertaken.

$W_2(CH_2Ph)_2$(EtCCEt$)_2$(O-*i*-Pr$)_4$. In a Schlenk reaction vessel, $W_2(CH_2Ph)_2(O\text{-}i\text{-}Pr)_4$ (430 mg, 0.55 mmol) was dissolved in hexane (20 mL) and cooled to 0 °C. 3-Hexyne (2.1 equiv, 130 μL, 1.15 mmol) was added to the cooled, red-brown hexane solution via microliter syringe. The mixture quickly turned to lime green and then to burnt orange. The solution was then stirred at room temperature for 45 min, concentrated to ca. 5 mL, and cooled to −20 °C for 24 h. Orange-brown, cubic crystals were harvested by removing the supernatant liquid via cannula and drying in vacuo (crystalline yield 375 mg, 72%).

IR data (Nujol mull between CsI plates, cm^{-1}): 1596 (s), 1571 (w), 1489 (s), 1332 (m), 1200 (m), 1166 (m), 1131 (s), 1112 (vs), 1058 (w), 1039 (w), 1029 (w), 1015 (s), 990 (vs), 974 (vs), 959 (vs), 856 (m), 847 (w), 837 (m), 800 (w), 755 (s), 728 (m), 698 (s), 592 (w), 568 (w), 452 (m).

Anal. Calcd for $W_2O_4C_{38}H_{62}$: C, 48.0; H, 6.5; N, 0.0. Found: C, 47.6, H, 6.4; N, 0.1.

Table XII. Alkyne Rotational Barriers in 1,2-$W_2(C_6H_4$-*p*-Me$)_2$(MeCCMe$)_2$(O-*t*-Bu$)_4$ (2′) and 1,2-W_2R_2(R′CCR′$)_2$(O-*i*-Pr$)_4$ (2)[a]

compd	R	R′	$T_{coal.}$ (°C)	$\Delta G^{\ddagger}$ (kcal mol^{-1})
2′	C_6H_4-*p*-Me	Me	35	14.4 ± 0.1
2	CH_2Ph	Me	−65	9.9 ± 0.1
2	*n*-Pr	Me	−77	9.1 ± 0.2
2	C_6H_4-*p*-Me	Me	−50	10.3 ± 0.2
2	CH_2SiMe_3	Me	−68	9.7 ± 0.1
2	Me	Me	−80	8.9 ± 0.2
2	C_6H_5	Me	−50	10.3 ± 0.1
2	CH_2SiMe_3	Et	−68	10.1 ± 0.2
2	CH_2Ph	Et	−59	10.3 ± 0.2

[a] Rotational barriers were calculated from coalescence temperatures by using the Gutowsky–Holm equation. See ref 55, pp 79, 109.

Table XIII. Electronic Absorption Data for 1,2-W_2R_2(R′CCR′$)_2$(O-*i*-Pr$)_4$ Compounds (2)

compound	λ (nm)	ν (cm^{-1})	(M^{-1} cm^{-1})[a]
2, R = CH_2Ph, R′ = Et	272	36 800	27 000
	330 (sh)	30 300	8 500
	380	26 300	8 100
	460 (sh)	21 700	2 600
	655	15 300	220
2, R = CH_2Ph, R′ = Me	268	37 300	25 000
	374	26 700	8 000
	460 (sh)	21 700	2 500
	640 (sh)	15 600	150
2, R = *n*-Pr, R′ = Me	240 (sh)	41 700	20 000
	340 (sh)	29 400	2 700
	410	24 400	2 700
	625 (sh)	16 000	62
2, R = CH_2SiMe_3, R′ = Me	340 (sh)	29 400	2 500
	408	24 500	3 000
	470	21 300	2 600
	650 (sh)	15 400	100

[a] The extinction coefficients have errors of ±10% based on errors in weighing and dilutions.

$W_2(CH_2SiMe_3)_2$(EtCCEt$)_2$(O-*i*-Pr$)_4$. A procedure similar to that described for $W_2(CH_2Ph)_2(EtCCEt)_2(O\text{-}i\text{-}Pr)_4$ was followed. $W_2(CH_2SiMe_3)_2(O\text{-}i\text{-}Pr)_4$ (400 mg, 0.51 mmol) was used to produce the orange crystalline product (crystalline yield 129 mg, 29%). No lime green color was observed when 3-hexyne was added.

IR data (KBr pellet, cm^{-1}): 2984 (vs), 2966 (s), 2951 (s), 2937 (m), 1460 (m), 1450 (m), 1380 (m), 1368 (s), 1330 (w), 1250 (s), 1241 (s), 1164 (m), 1130 (s), 1111 (vs), 991 (s), 968 (s), 952 (s), 850 (s), 837 (vs), 825 (m), 751 (vw), 720 (w), 693 (vw), 681 (vw), 669 (vw), 582 (w), 547 (vw), 500 (w), 418 (vw).

Anal. Calcd for $W_2O_4C_{32}Si_2H_{70}$: C, 40.8; H, 7.4; N, 0.0. Found: C, 40.2; H, 7.3; N, <0.03.

W_2Me_2(EtCCEt$)_2$(O-*i*-Pr$)_4$. In a Schlenk reaction vessel, $W_2Me_2(NMe_2)_4$ (300 mg, 0.52 mmol) was dissolved in pentane (15 mL) and cooled to 0 °C. 3-Hexyne (2.1 equiv, 125 μL) was added to the yellow solution resulting in no apparent color change. *i*-PrOH (4.1 equiv, 170 μL) was then added at 0 °C causing the color to quickly turn dark brown and then orange. The solution was stirred for 30 min at 0 °C. The reaction mixture was then concentrated to ca. 3 mL total volume and cooled to −20 °C for 12 h. Only small amounts of $[(EtC{\equiv})W(O\text{-}i\text{-}Pr)_3(HNMe_2)]_2$[29] crystallized from solution. ^1H NMR analysis of the filtrate revealed a ca. 3:1 ratio of $W_2Me_2(EtCCEt)_2(O\text{-}i\text{-}Pr)_4$ to $(EtC{\equiv})W(O\text{-}i\text{-}Pr)_3(HNMe_2)$, respectively. Further attempts to separate the compounds by fractional crystallization were unsuccessful.

$W_2(C_6H_4$-*p*-Me$)_2$(MeCCMe$)_2$(O-*t*-Bu$)_4$. A procedure identical with that described for $W_2(CH_2Ph)_2(MeCCMe)_2(O\text{-}i\text{-}Pr)_4$ was

followed. $W_2(p\text{-tolyl})_2(O\text{-}t\text{-Bu})_4$ (250 mg, 0.30 mmol) was used to produce the orange-brown crystalline product. A dark gray color was transiently observed after the solution was warmed to room temperature (crystalline yield 145 mg, 51%).

IR data (KBr pellet, cm^{-1}): 3045 (w), 2975 (s), 2922 (s), 2895 (m), 2860 (m), 1625 (m, br), 1481 (w), 1453 (m), 1385 (s), 1361 (s), 1354 (m), 1258 (w), 1233 (m), 1178 (m), 1162 (vs), 1021 (w), 1012 (w), 958 (vs), 888 (m), 859 (s), 800 (m), 790 (w), 753 (m), 681 (w), 560 (m), 551 (m), 504 (w), 440 (w), 370 (vw).

Anal. Calcd for $W_2O_4C_{38}H_{62}$: C, 48.01; H, 6.57. Found: C, 48.31; H, 6.85.

$[W(\equiv CEt)(CH_2\text{-}t\text{-Bu})(O\text{-}i\text{-Pr})_2]_2$. In a Schlenk reaction vessel, $W_2(CH_2\text{-}t\text{-Bu})_2(O\text{-}i\text{-Pr})_4$ (406 mg, 0.54 mmol) was dissolved in pentane (12 mL) and cooled to 0 °C. 3-Hexyne (1.1 equiv, 0.59 mmol, 68 μL) was added via microliter syringe, and the orange solution faded to pale brown. The reaction mixture was filtered through a fine frit and the filtrate concentrated to ca. 3 mL and cooled to −20 °C. After 24 h, large pale yellow cubes were harvested by removing the supernatant liquid via cannula and drying in vacuo (crystalline yield 296 mg, 64%).

$[W(\equiv CEt)(CH_2\text{-}t\text{-Bu})(O\text{-}i\text{-Pr})_2(py)]_2$. In a Schlenk reaction vessel, $W_2(CH_2\text{-}t\text{-Bu})_2(O\text{-}i\text{-Pr})_4$ (400 mg, 0.53 mmol) was dissolved in hexane (12 mL) and cooled to 0 °C. 3-Hexyne (1.0 equiv, 0.53 mmol, 61 μL) was added to the 0 °C orange hexane solution by using a microliter syringe. The color slowly faded to pale brown over a 5-min period. Excess pyridine (1.0 mL, 12.4 mmol) was added via a syringe causing the solution to darken slightly. The mixture was stirred at 0 °C for an additional 45 min. The solution was then concentrated to ca. 2 mL and cooled to −20 °C. After 48 h, ca. 150 mg of oily brown crystals were harvested by removing the supernatant liquid via cannula and drying in vacuo (approximate yield 29%). The crystalline material turned into a brown oil after 20 min at 25 °C.

1,1-$W_2Me_2(\mu\text{-MeCCMe})(O\text{-}t\text{-Bu})_4(py)$. In a Schlenk reaction vessel, 1,2-$W_2Me_2(O\text{-}t\text{-Bu})_4(py)_2$ (525 mg, 0.62 mmol) was dissolved in pentane (10 mL) and the resulting burgundy solution frozen at −198 °C. 2-Butyne (1 equiv, 0.62 mmol) was condensed into the flask by using a calibrated vacuum manifold. The mixture was quickly warmed to 0 °C in an ice–water bath during which time the burgundy solution rapidly turned royal blue. The solution was stirred for 10 min at 0 °C, concentrated to ca. 3 mL, and cooled to −20 °C for 12 h. Large blue crystals were isolated at −78 °C by removing the supernatant liquid via cannula and drying in vacuo (crystalline yield 250 mg, 49%).

$W_2Me(\mu\text{-HCCH})(O\text{-}t\text{-Bu})_5(py)$. A Schlenk reaction vessel was charged with 1,2-$W_2Me_2(O\text{-}t\text{-Bu})_4(py)_2$ (512 mg, 0.60 mmol) and hexane (10 mL) and frozen at −198 °C. With use of a calibrated vacuum manifold, ethyne (1 equiv, 0.60 mmol) was condensed into the flask. The frozen, burgundy solution was rapidly warmed to 0 °C whereupon it turned dirty green. The solvent was removed in vacuo at 0 °C and the green residue extracted into dimethoxyethane (ca. 2 mL) and cooled to −20 °C. After 24 h, green needlelike crystals were harvested by removing the supernatant liquid via cannula and drying in vacuo (crystalline yield 90 mg, 18%).

IR data (KBr pellet, cm^{-1}): 2975 (s), 2925 (m), 2860 (w), 1601 (w), 1486 (w), 1470 (w), 1446 (m), 1383 (s), 1356 (s), 1232 (m), 1218 (w), 1178 (vs), 1069 (w), 1041 (w), 1022 (w), 970 (vs), 895 (m), 782 (m), 759 (w), 695 (w), 658 (w), 548 (m).

Anal. Calcd for $W_2O_5C_{28}H_{55}N$: C, 39.4; H, 6.5; N, 1.6. Found: C, 36.4; H, 5.9; N, 1.6. Calcd for $W_2O_5C_{26}H_{55}N$ (allowing for WC formation): C, 36.6; H, 6.5; N, 1.6.

1,2-$Mo_2R_2(O\text{-}i\text{-Pr})_4$ Compounds and Alkynes. Typical reactions involved ca. 0.08 mmol of 1,2-$Mo_2R_2(O\text{-}i\text{-Pr})_4$ (R = CH_2Ph or $CH_2\text{-}t\text{-Bu}$) dissolved in hexane (10 mL) in Schlenk reaction vessels. The orange-yellow hexane solutions were frozen at −198 °C, and excess alkyne (>3 equiv of HCCH or MeCCMe) was condensed into the flask by using a calibrated vacuum manifold. The frozen mixtures were rapidly warmed to 0 °C in ice–water baths. Upon melting, copious amounts of black or purple-black precipitate rapidly formed in the flasks. The reaction mixtures were stirred for an additional 0.5 h at room temperature. The resulting slurries were evaporated to dryness and the soluble residues extracted into C_6D_6 producing orange-yellow solutions. ^1H NMR analysis of these solutions revealed only unreacted 1,2-$Mo_2R_2(O\text{-}i\text{-Pr})_4$.

$W_2R_2(R'CCR'')_2(O\text{-}i\text{-Pr})_4$ + CO, PMe_3, and Acetylenes. Reactions between $W_2R_2(R'CCR'')_2(O\text{-}i\text{-Pr})_4$ and CO were run in NMR tubes fitted with septum caps. Typically 0.025 mmol of compound was dissolved in C_6D_6 (0.5 mL) in a drybox. The solutions were then cooled to 0 °C and carbon monoxide syringed into the NMR tube headspace by using a gas-tight syringe. Samples were analyzed by ^1H NMR spectroscopy. After 4 h, no apparent reactions had occurred.

Reactions between $W_2R_2(R'CCR'')_2(O\text{-}i\text{-Pr})_4$ and PMe_3 were run in sealed NMR tubes in C_6D_6. Approximately 0.025 mmol of compound was dissolved in C_6D_6 (0.5 mL) in an extended NMR tube. The samples were frozen to −198 °C, and PMe_3 (ca. 2 equiv) was condensed into the tube by using a calibrated vacuum manifold. The tubes were then sealed with a torch and warmed to room temperature. After 24 h, only starting material and free PMe_3 were detected by ^1H NMR.

Reactions between $W_2R_2(R'CCR'')_2(O\text{-}i\text{-Pr})_4$ and acetylenes (MeC≡CMe or HC≡CH) were run in hexane solvent (ca. 5 mL) in Schlenk flasks employing 0.025 mmol of material. The hexane solutions were frozen at −198 °C, and acetylene (usually about 2 equiv) was condensed into the flask by using a calibrated vacuum manifold. The frozen mixtures were rapidly warmed to 0 °C and stirred at room temperature for ca. 2 h. Copious amounts of black or dark purple precipitate began to form after 10–20 min. After being stirred for ca. 2 h, the mixtures were evaporated to dryness and the soluble components of the dark residues extracted into C_6D_6 (0.5 mL). ^1H NMR analysis of the resulting C_6D_6 solutions revealed only unreacted $W_2R_2(R'CCR'')_2(O\text{-}i\text{-Pr})_4$.

Crystallographic Studies. General operating procedures and listings of programs have been previously given.[56]

$W_2(CH_2Ph)_2(O\text{-}i\text{-Pr})_4(MeCCMe)_2$. A suitable fragment was cleaved from a larger crystal and transferred to the goniostat by using standard inert-atmosphere handling techniques employed by the Indiana University Molecular Structure Center.

A search of a limited hemisphere of reciprocal space located a set of diffraction maxima with monoclinic symmetry and extinctions corresponding to the unique space group $P2_1/n$ (an alternate setting of $P2_1/c$). Data were collected in the usual manner and corrected for absorption as well as Lorentz and polarization terms.

The two tungsten atoms were located in a Patterson synthesis (using TRISH), and all other atoms were located in two subsequent difference Fouriers. All hydrogen atoms were located and refined isotropically, and all non-hydrogen atoms were varied anisotropically.

A final difference Fourier was featureless, the largest peak being 0.48 e/Å^3.

$W_2(Ph)_2(O\text{-}i\text{-Pr})_4(MeCCMe)_2$. A suitable small orange crystal fragment was selected, transferred to the goniostat, cooled to −159 °C and characterized in the usual manner. A systematic search of a limited hemisphere of reciprocal space yielded a set of reflections which exhibited monoclinic symmetry and extinctions corresponding to the space group $P2_1/n$.

The structure was solved by locating the heavy atoms by direct methods and the remaining atoms in a difference Fourier phased by the W atoms. Almost all hydrogen atoms were located in a difference map following initial refinement. All hydrogen atoms were included in fixed positions, and the full-matrix least-squares refinement was completed by using anisotropic thermal parameters on all non-hydrogen atoms. The data were corrected for absorption. A total of 3803 reflections having $F > 3.0\sigma(F)$ were used in the refinements.

The final difference map was essentially featureless, a few peaks of ca. 1 e/Å^3 were located close to heavy atoms.

The purple crystals were also examined and found to be $W_2(Ph)_2(O\text{-}i\text{-Pr})_3(NMe_2)(HNMe_2)(\mu\text{-}C_2Me_2)$, a product presumably arising from incomplete alcoholysis in the preparation of $W_2(Ph)_2(O\text{-}i\text{-Pr})_4$. The details of this structure will be presented elsewhere.

$[W(\equiv CEt)(O\text{-}i\text{-Pr})_2(CH_2\text{-}t\text{-Bu})]_2$. A suitable crystal was located and transferred to the goniostat by using standard inert-atmosphere handling techniques employed by the Indiana

(56) Chisholm, M. H.; Folting, K.; Huffman, J. C.; Kirkpatrick, C. C. *Inorg. Chem.* **1984**, *23*, 1021.

University Molecular Structure Center and cooled to −155 °C for characterization and data collection.

A systematic search of a limited hemisphere of reciprocal space located a set of diffraction maxima with no systematic absences or symmetry, leading to the choice of a triclinic space group. Subsequent solution and refinement of the structure confirmed the centric choice ($P\bar{1}$).

Most of the hydrogen atom positions were visible in a difference Fourier phased on the non-hydrogen parameters. When the hydrogen atoms were allowed to vary, those associated with the isopropyl group on O(14) tended to not converge, so for this reason, the positions of all hydrogens were calculated and placed in fixed idealized (d(C–H) = 0.95 Å) for the final cycles. The hydrogen atoms were assigned a thermal parameter of 1 + B_{iso} of the carbon atom to which they were bound.

A final difference Fourier was essentially featureless, with the largest peak being 0.50 e/Å^3, other than two peaks of intensity 1.4 e/Å^3 located adjacent to the tungsten atom position. The tungsten–tungsten distance is 3.514 (1) Å.

W_2(Me)$_2$(O-*t*-Bu)$_4$(py)(MeCCMe). The sample consisted of large intergrown crystals, and a suitable sample was eventually cleaved from a larger crystal and transferred to the goniostat where it was cooled to −165 °C for characterization and data collection. A systematic search of a limited hemisphere of reciprocal space revealed a set of diffraction maxima which could be indexed as monoclinic, space group $P2_1/c$. Subsequent solution and refinement confirmed the choice.

The structure was solved by a combination of direct methods (MULTAN78) and Fourier techniques and refined by full-matrix least squares. The bridging O-*t*-Bu group was found to be disordered, and refinement of the occupancies indicate an approximate 50:50 ratio of the two alternate sites. The occupancies were thus fixed at 0.50 for the final cycles, and the various figures show only the one set of methyls. Hydrogen atoms were present for most of the atoms, and the located positions were used to calculate fixed positions which were used in the remainder of the refinement.

A final difference Fourier was featureless except for peaks of 1.34 and 1.20 e/Å^3 located at the two metal sites. All other peaks were less than 1.0 e/Å^3. Because of the poor shape of the crystal no absorption correction was made. A ψ scan of two reflections indicated less than 10% variance.

Acknowledgment. We thank the National Science Foundation for financial support. B.W.E. was the Indiana University SOHIO graduate fellow, 1985–1987.

Registry No. 1 (R = CH_2SiMe_3), 116563-40-7; 1 (R = CH_2Ph), 99639-27-7; 1 (R = CH_2-*t*-Bu), 101860-13-3; **2** (R = CH_2Ph, R′ = Me), 116563-26-9; **2** (R = CH_2SiMe_3, R′ = Me), 116563-27-0; **2** (R = R′ = Me), 116563-28-1; **2** (R = *n*-Pr, R′ = Me), 110433-53-9; **2** (R = *i*-Bu, R′ = Me), 110456-68-3; **2** (R = Et, R′ = Me), 116563-29-2; **2** (R = C_6H_5, R′ = Me), 116563-30-5; **2** (R = C_6H_4-*p*-Me, R′ = Me), 116563-31-6; **2** (R = CH_2Ph, R′ = Me, R″ = Et), 116595-62-1; **2** (R = *n*-Pr, R′ = Me, R″ = Et), 116563-32-7; **2** (R = CH_2Ph, R′ = Et), 116563-33-8; **2** (R = CH_2SiMe_3, R′ = Et), 116563-34-9; **2** (R = Me, R′ = Et), 116563-35-0; **2′** (R = C_6H_4-*p*-Me, R′ = Me), 116563-36-1; **4**, 116563-37-2; **5**, 116595-64-3; **6**, 116563-38-3; $W_2Cl_2(NMe_2)_4$, 63301-81-5; $W_2(C_6H_4$-*p*-Me$)_2$(O-*t*-Bu$)_4$, 110348-82-8; $W_2(C_6H_4$-*p*-Me$)_2(NMe_2)_4$, 84417-28-7; W_2(O-*t*-Bu$)_6$, 57125-20-9; $W_2Me_2(NMe_2)_4$, 72286-64-7; [(MeC≡)W(O-*i*-Pr$)_3$(HNMe$_2$)]$_2$, 116595-63-2; W_2(*i*-Pr$)_2(NMe_2)_4$, 72286-68-1; W_2(*n*-Pr$)_2(NMe_2)_4$, 116563-41-8; W_2(*i*-Bu$)_2(NMe_2)_4$, 101860-16-6; W_2Me(*μ*-HCCH)(O-*t*-Bu$)_5$(py), 116563-39-4; $W_2Et_2(NMe_2)_4$, 72286-65-8; $W_2(C_6H_5)_2$(O-*i*-Pr$)_4$(HNMe$_2$), 101915-85-9; W_2(C_6H_4-*p*-Me$)_2$(O-*i*-Pr$)_4$(HNMe$_2$), 101915-86-0; [(EtC≡)W(O-*i*-Pr$)_3$(HNMe$_2$)]$_2$, 104240-17-7; W_2Me_2(O-*t*-Bu$)_4$(py)$_2$, 101860-11-1; 1,2-$Mo_2(CH_2Ph)_2$(O-*i*-Pr$)_4$, 91443-57-1; 1,2-$Mo_2(CH_2$-*t*-Bu$)_2$(O-*i*-Pr$)_4$, 101859-82-9; $LiCH_2SiMe_3$, 1822-00-0.

Supplementary Material Available: For $W_2(CH_2Ph)_2$(O-*i*-Pr$)_4$(MeCCMe$)_2$, W_2(Ph$)_2$(O-*i*-Pr$)_4$(MeCCMe$)_2$, W_2Me_2(O-*t*-Bu$)_4$(py)(MeCCMe), and [W(≡CEt)(O-*i*-Pr$)_2$(CH_2-*t*-Bu)]$_2$, tables of anisotropic thermal parameters and complete listing of bond distances and angles and stereodrawings (38 pages); listings of F_o and F_c values (51 pages). Ordering information is given on any current masthead page.